

GNNX-BENCH: Unravelling the Utility of Perturbation-based GNN Explainers through In-depth Benchmarking

Mert Kosan^{*†}

Visa Research, Austin
mertkosan@gmail.com

Samidha Verma^{*}

Indian Institute of Technology, Delhi
samidha.verma@cse.iitd.ac.in

Burouj Armgaan

Indian Institute of Technology, Delhi
burouj.armgaan@cse.iitd.ac.in

Khushbu Pahwa

Rice University
kp66@rice.edu

Ambuj Singh

University of California, Santa Barbara
ambuj@cs.ucsb.edu

Sourav Medya

University of Illinois, Chicago
medya@uic.edu

Sayan Ranu

Indian Institute of Technology, Delhi
sayanranu@cse.iitd.ac.in

Abstract

Numerous explainability methods have been proposed to shed light on the inner workings of GNNs. Despite the inclusion of empirical evaluations in all the proposed algorithms, the interrogative aspects of these evaluations lack diversity. As a result, various facets of explainability pertaining to GNNs, such as a comparative analysis of counterfactual reasoners, their stability to variational factors such as different GNN architectures, noise, stochasticity in non-convex loss surfaces, feasibility amidst domain constraints, and so forth, have yet to be formally investigated. Motivated by this need, we present a benchmarking study on perturbation-based explainability methods for GNNs, aiming to systematically evaluate and compare a wide range of explainability techniques. Among the key findings of our study, we identify the Pareto-optimal methods that exhibit superior efficacy and stability in the presence of noise. Nonetheless, our study reveals that all algorithms are affected by stability issues when faced with noisy data. Furthermore, we have established that the current generation of counterfactual explainers often fails to provide feasible recourses due to violations of topological constraints encoded by domain-specific considerations. Overall, this benchmarking study empowers stakeholders in the field of GNNs with a comprehensive understanding of the state-of-the-art explainability methods, potential research problems for further enhancement, and the implications of their application in real-world scenarios.

1 Introduction and Related Work

GNNs have shown state-of-the-art performance in various domains including social networks [32, 13], drug discovery [56, 35, 36], modeling of physical systems [44, 8, 9, 10], event detection [12, 25], and recommendation engines [58]. Unfortunately, like other deep-learning models, GNNs are black boxes due to lacking transparency and interpretability. This lack of interpretability is a significant barrier to their adoption in critical domains such as healthcare, finance, and law enforcement. In addition, the ability to explain predictions is critical towards understanding potential flaws in the model and generate insights for further refinement. To impart interpretability to GNNs, several algorithms to explain the inner workings of GNNs have been proposed. The diversified landscape of GNN explainability research is visualized in Fig. 1. We summarize each of the categories below:

^{*}Both authors contributed equally to this research.

[†]Disclaimer: Mert Kosan worked on this project prior to joining Visa Research.

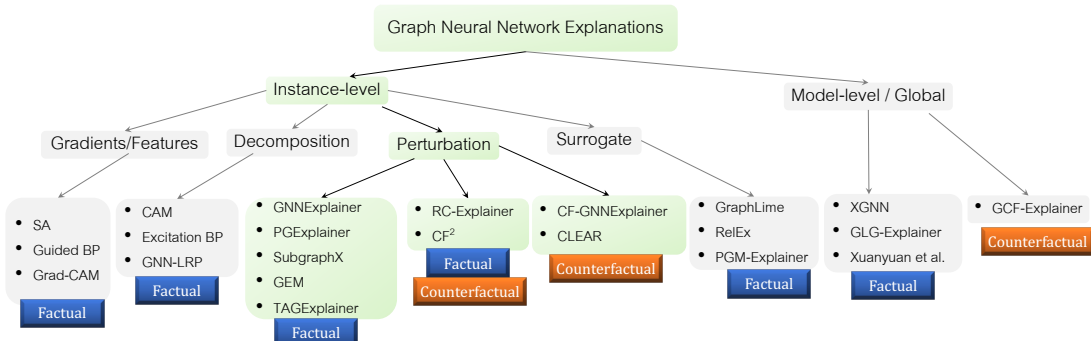


Figure 1: Structuring the space of the existing methods on GNN explainability as follows. **Gradient:** SA [7], Guided-BP [7], Grad-CAM [33]; **Decomposition:** Excitation-BP [33], GNN-LRP [38], CAM [33]; **Perturbation:** GNNExplainer [59], PGExplainer [30], SubgraphX [62], GEM [27], TAGExplainer [51], CF² [43], RCExplainer [6], CF-GNNExplainer [29], CLEAR [31]; **Surrogate:** GraphLime [18], RelEx [64], PGM-Explainer [47]; **Global:** XGNN [60], GLG-Explainer [5], Xuanyuan et al. [54], GCFExplainer [19].

- **Model-level:** Model-level or global explanations [60, 19, 54] are concerned about the overall behavior of the model and searches for patterns in the set of predictions made by the model.
- **Instance-level:** Instance-level or local explainers [59, 30, 40, 62, 18, 61, 29, 43, 27, 6, 1, 50] provide explanations for specific predictions made by a model. For instance, these explanations reason about why a particular instance or input is classified or predicted in a certain way.
- **Gradient-based:** The gradient-based explainers [33, 7] follow the idea of the rate of change being represented by gradients. Additionally, the gradient of the prediction with respect to the input represents the sensitivity of the prediction with respect to the input. This sensitivity gives the importance scores and helps in finding explanations.
- **Decomposition-based:** These explainers [33, 7, 39, 38] consider the prediction of the model to be decomposed and distributed backwards in a layer by layer fashion and the score of different parts of the input can be construed as its importance to the prediction.
- **Perturbation-based:** These methods [59, 30, 62, 18, 29, 43, 27, 6, 31, 1, 50] utilize perturbations of the input to identify important subgraphs that serve as factual or counterfactual explanations.
- **Surrogate:** Surrogate methods [64, 47, 18] use the generic intuition that in a smaller range of input values, the relationship between input and output can be approximated by interpretable functions. The methods fit a simple and interpretable surrogate model in the locality of the prediction.

In addition to the methodology employed by explanation algorithms, the type of explanation offered represents a crucial component. Explanations can be broadly classified into two categories: *factual* reasoning [59, 30, 40, 62, 18] and *counterfactual* reasoning [29, 43, 31, 6, 1, 50].

- **Factual explanations** provide insights into the rationale behind a specific prediction by identifying the minimal subgraph that is sufficient to yield the same prediction as the entire input graph.
- **Counterfactual explanations**, on the other hand, elucidate why a particular prediction was not made by presenting alternative scenarios that could have resulted in a different decision. In the context of graphs, this involves identifying the smallest perturbation to the input graph that alters the prediction of the GNN. Perturbations typically involves the removal of edges or modifications to node features. Counterfactual reasoners possess an additional advantage compared to factual reasoning, as they provide a recourse mechanism [46]. For instance, in the domain of drug discovery [21, 52], mutagenicity represents an undesirable property that impedes a molecule’s potential as a drug [23]. While factual explainers can attribute the subgraph responsible for mutagenicity, counterfactual reasoners can identify this subgraph along with the alterations required to render the molecule non-mutagenic.

1.1 Existing Benchmarking Studies on GNN Explainability

GraphFrameX [4] and GraphXAI [2] represent two notable benchmarking studies. While both investigations have contributed valuable insights into GNN explainers, certain unresolved investigative aspects persist.

- **Inclusion of counterfactual explainability:** GraphFrameX and GraphXAI have focused on factual explainers for GNNs. [34] has discussed methods and challenges, but benchmarking on counterfactual explainers remains underexplored.
- **Achieving Comprehensive coverage:** Existing literature encompasses seven perturbation-based factual explainers. However, GraphFrameX and GraphXAI collectively assess only GnnExplainer [59], PGExplainer [30], and SubgraphX [62].

Table 1: Key highlights of the *perturbation-based* factual methods. The “NFE” column implies *Node Feature Explanation*. “GC” and “NC” indicate whether the dataset is used for graph classification and node classification respectively.

Method	Subgraph Extraction Strategy	Scoring function	Constraints	NFE	Task	Nature
GNNExplainer [57]	Continuous relaxation	Mutual Information	Size	Yes	GC+NC	Transductive
PGExplainer [30]	Parameterized edge selection	Mutual Information	Size and/or connectivity	No	GC+NC	Inductive
TAGExplainer [51]	Sampling	Mutual Information	Size, Entropy	No	GC+NC	Inductive
GEM [27]	Granger Causality+Autoencoder	Causal Contribution	Size, Connectivity	No	GC+NC	Inductive
SubgraphX [62]	Monte Carlo Tree Search	Shapley Value	Size, connectivity	No	GC	Transductive
GstarX [63]	Monte Carlo sampling	HN-value	Size	No	GC	Inductive

- **Empirical investigations:** How susceptible are the explanations to topological noise, variations in GNN architectures, or optimization stochasticity? Do the counterfactual explanations provided align with the structural and functional integrity of the underlying domain? To what extent do these explainers elucidate the GNN model as opposed to the underlying data? Are there standout explainers that consistently outperform others in terms of performance? These are critical empirical inquiries that necessitate attention.

1.2 Contributions

In this benchmarking study, we systematically study perturbation-based factual and counter-factual explainers and identify their strengths and limitations in terms of their ability to provide accurate, meaningful, and actionable explanations for GNN predictions. Overall, we make the following key contributions:

- **Comprehensive evaluation encompassing counterfactual explainers:** The benchmarking study encompasses seven factual explainers and four counterfactual explainers. The proposed work is the first benchmarking study on counterfactual explainers for GNNs.
- **Novel insights:** The findings of our benchmarking study unveil stability to noise and variational factors, and generating feasible counterfactual recourses as two critical technical deficiencies that naturally lead us towards open research challenges.
- **Codebase:** As a by-product, a meticulously curated, publicly accessible code base is provided (<https://github.com/Armagaan/gnn-x-bench>).

To keep the benchmarking study focused, we investigate only the perturbation-based explainability methods (highlighted in green in Fig. 1). While model-level explainers operate on the GNN model, other forms of instance-level explainers yield diverse outputs spanning Directed Acyclic Graphs in PGMEExplainer [47], model weights in Graph-Lime [18], node sets in Grad-CAM [33], among others. Consequently, enforcing a standardized set of inquiries across all explainers is not meaningful.

2 Preliminaries and Background

We use the notation $\mathcal{G} = (\mathcal{V}, \mathcal{E})$ to represent a graph, where \mathcal{V} denotes the set of nodes and \mathcal{E} denotes the set of edges. Each node $v_i \in \mathcal{V}$ is associated with a feature vector $x_i \in \mathbb{R}^d$. We assume there exists a GNN Φ that has been trained on \mathcal{G} (or a set of graphs). Existing works has predominantly assumed the GNN model Φ to be a message-passing architecture such as GCN [24], GRAPHsAGE [17], GAT [45], and GIN [53]. Therefore, we will base our subsequent discussion on this assumption.

The literature on GNN explainability has primarily focused on *graph classification* and *node classification*, and hence the output space is assumed to be categorical. In graph classification, we are given a set of graphs as input, each associated with a class label. The task of the GNN Φ is to correctly predict this label. In the case of node classification, class labels are associated with each node and the predictions are performed on nodes. In a message passing GNN of ℓ layers, the embedding on a node is a function of its ℓ -hop neighborhood. We use the term *inference subgraph* to refer to this ℓ -hop neighborhood. Hence forth, we will assume that graph refers to the inference subgraph for node classification. Factual and counterfactual reasoning over GNNs are defined as follows.

Definition 1 (Perturbation-based Factual Reasoning) *Let \mathcal{G} be the input graph and $\Phi(\mathcal{G})$ the prediction on \mathcal{G} . Our task is to identify the smallest subgraph $\mathcal{G}_S \subseteq \mathcal{G}$ such that $\Phi(\mathcal{G}) = \Phi(\mathcal{G}_S)$. Formally, the optimization problem is expressed as follows:*

$$\mathcal{G}_S = \arg \min_{\mathcal{G}' \subseteq \mathcal{G}, \Phi(\mathcal{G}') = \Phi(\mathcal{G})} \|\mathcal{A}(\mathcal{G}_S)\| \quad (1)$$

Here, $\mathcal{A}(\mathcal{G}_S)$ denotes the adjacency matrix of \mathcal{G}_S , and $\|\mathcal{A}(\mathcal{G}_S)\|$ is its L1 norm which is equivalent to the number of edges. Note that if the graph is undirected, the number of edges is half of the L1 norm. Nonetheless, the optimization problem remains the same.

Table 2: Key highlights of the counterfactuals methods. “GC” and “NC” indicate whether the dataset is used for graph classification and node classification respectively.

Method	Explanation Type	Task	Target/Method	Nature
RCExplainer [6]	Instance level	GC+NC	Neural Network	Inductive
CF ² [43]	Instance level	GC+NC	Original graph	Transductive
CF-GNNExplainer [29]	Instance level	NC	Inference subgraph	Transductive
CLEAR [31]	Instance level	GC+NC	Variational Autoencoder	Inductive

While subgraph generally concerns only the topology of the graph, since graphs in our case may be annotated with features, some algorithms formulate the minimization problem in the joint space of topology and features. Specifically, in addition to identifying the smallest subgraph, we also want to minimize the number of features required to characterize the nodes in this subgraph.

Definition 2 (Counterfactual Reasoning) Let \mathcal{G} be the input graph and $\Phi(\mathcal{G})$ the prediction on \mathcal{G} . Our task is to introduce the minimal set of perturbations to form a new graph \mathcal{G}^* such that $\Phi(\mathcal{G}) \neq \Phi(\mathcal{G}^*)$. Mathematically, this entails to solving the following optimization problem.

$$\mathcal{G}^* = \arg \min_{\mathcal{G}' \in \mathbb{G}, \Phi(\mathcal{G}) \neq \Phi(\mathcal{G}')} \text{dist}(\mathcal{G}, \mathcal{G}') \quad (2)$$

where $\text{dist}(\mathcal{G}, \mathcal{G}')$ quantifies the distance between graphs \mathcal{G} and \mathcal{G}' and \mathbb{G} is the set of all graphs one may construct by perturbing \mathcal{G} .

Typically, distance is measured in terms of number of edge perturbations while keeping the node set fixed. Under this assumption, $\text{dist}(\mathcal{G}, \mathcal{G}')$ and \mathbb{G} are defined as:

$$\begin{aligned} \mathbb{G} &= \{\mathcal{G}'(\mathcal{V}, \mathcal{E}') \mid \mathcal{E}' \subseteq \mathcal{V} \times \mathcal{V}\} \\ \text{dist}(\mathcal{G}, \mathcal{G}') &= \|\mathcal{A}_{\mathcal{G}} - \mathcal{A}_{\mathcal{G}'}\| \end{aligned}$$

where $\mathcal{A}_{\mathcal{G}}$ denotes as adjacency matrix of \mathcal{G} .

2.1 Review of Perturbation-based GNN Reasoning

Factual [61, 22]: The perturbation schema for factual reasoning usually consists of two crucial components: the subgraph extraction module and the scoring function module. Given an input graph \mathcal{G} , the subgraph extraction module extracts a subgraph \mathcal{G}_s ; and the scoring function module evaluates the model predictions $\Phi(\mathcal{G}_s)$ for the subgraphs, comparing them with the actual predictions $\Phi(\mathcal{G})$. For instance, **GNNExplainer** [57] identifies an explanation in the form of a subgraph that have the maximum influence on the prediction. In a follow-up work, **PGExplainer** [30] extends the same idea with an additional assumption of the graph to be a random Gilbert graph. Unlike the existing explainers, **TAGExplainer** [51] takes a two-step approach where the first step has an embedding explainer trained using a self-supervised training framework without any information of the downstream task. A causality-based method **GEM** [27] uses the *Granger causality* to generate ground-truth explanations which are used to train the explainer. **SubgraphX** [62] and **GStarX** [63] use cooperative game theoretic techniques. In particular, SubgraphX applies the Shapley value [41] to measure the importance of the subgraphs and GStarX uses HN values [16], to compute importance scores of a node for both graph and node classification tasks. Table 1 summarizes the key highlights. **Counterfactual [61, 22]:** **CF-GNNExplainer** [29] aims to perturb the computational graph by using a binary mask matrix. The corresponding loss function quantifies the accuracy of the produced counterfactual, and captures the distance (or similarity) between the counterfactual graph and the original graph. In follow-up work, **CF²** [43] extends this method by including a contrastive loss that jointly optimizes the quality of both the factual and the counterfactual explanation. **RCExplainer** [6], being both factual and counterfactual method, aims to identify a resilient subset of edges to remove such that it alters the prediction of the remaining graph. Finally **CLEAR** [31] generates counterfactual graphs by using a graph variational autoencoder. Table 2 summarizes the key highlights.

3 Benchmarking Framework

In this section, we outline the investigations we aim to conduct and the rationale behind them.

Comparative Analysis: We evaluate algorithms for both factual and counterfactual reasoning across a set of carefully chosen benchmark datasets (§ 4). Based on our holistic evaluation, we identify the pareto-optimal methods in terms of their performance, elucidating the trade-offs between different explainability techniques.

Stability: Stability of explanations, when faced with minor variations in the evaluation framework, is a crucial aspect that ensures their reliability and trustworthiness. Stability is quantified by taking the *Jaccard similarity* between the set of edges in the original explanation vs. those obtained after introducing the variation (details in § 4). In order to evaluate this aspect, we consider the following perspectives:

Table 3: The statistics of the datasets. Here, “F” and “CF” in the column “X-type” indicates whether the dataset is used for Factual or Counterfactual reasoning. “GC” and “NC” in the *Task* column indicates whether the dataset is used for graph classification and node classification respectively.

	#Graphs	#Nodes	#Edges	#Features	#Classes	Task	F/CF
MUTAGENICITY [37, 23]	4337	131488	133447	14	2	GC	F+CF
PROTEINS [11, 15]	1113	43471	81044	32	2	GC	F+CF
IMDB-B [55]	1000	19773	96531	136	2	GC	F+CF
AIDS [20]	2000	31385	32390	42	2	GC	F+CF
MUTAG [20]	188	3371	3721	7	2	GC	F+CF
NCI1 [48]	4110	122747	132753	37	2	GC	F
GRAPH-SST2 [61]	70042	714325	644283	768	2	GC	F
DD [15]	1178	334925	843046	89	2	GC	F
REDDIT-B [55]	2000	859254	995508	3063	2	GC	F
OGBG-MOLHIV [3]	41127	1049163	2259376	9	2	GC	CF
TREE-CYCLES [57]	1	871	1950	10	2	NC	CF
TREE-GRID [57]	1	1231	3410	10	2	NC	CF
BA-SHAPES [57]	1	700	4100	10	4	NC	CF

- **Perturbations in topological space:** If we inject minor perturbations to the topology through a small number of edge deletions or additions, then that should not affect the explanations.
- **Model parameters:** The explainers are deep-learning models themselves and optimize a non-convex loss function. As a consequence of non-convexity, when two separate instances of the explainer starting from different seeds are applied to the same GNN model, they generate dissimilar explanations. Our benchmarking study investigates the impact of this stochasticity on the quality and consistency of the explanations produced.
- **Model architectures:** Message-passing GNNs follow a similar computation framework, differing mainly in their message aggregation functions. We explore the stability of explanations under variations in the model architecture.

Necessity and Reproducibility: The objective in this experiment is to quantify how central the explanation subgraph is for the GNN towards making the prediction. We approach this question from the perspectives of necessity and reproducibility. Factual explanations are *necessary* if the removal of the explanation subgraph from the graph results in a significant decrease in prediction accuracy. Reproducibility [26], on the other hand, measures if the GNN is retained on the residual graph following the removal of the explanation, can it recover the original prediction?

Feasibility: One notable characteristic of counterfactual reasoning is its ability to offer recourse options. Nonetheless, in order for these recourses to be effective, they must adhere to the specific domain constraints. For instance, in the context of molecular datasets, the explanation provided must correspond to a valid molecule. Likewise, if the domain involves consistently connected graphs, the recourse must maintain this property. The existing body of literature on counterfactual reasoning with GNNs has not adequately addressed this aspect, a gap we address in our benchmarking study.

4 Empirical Evaluation

In this section, we execute the investigation plan outlined in § 3. Unless mentioned specifically, the base black-box GNN is a GCN. Details of the set up (e.g., hardware) are provided in App. A.

Datasets: Table 3 showcases the principal statistical characteristics of each dataset employed in our experiments, along with the corresponding tasks evaluated on them. The TREE-CYCLES, TREE-GRID, and BA-SHAPES datasets serve as benchmark graph datasets for counterfactual analysis. These datasets incorporate ground-truth explanations [43, 27, 29]. Each dataset contains an undirected base graph to which predefined motifs are attached to random nodes, and additional edges are randomly added to the overall graph. The class label assigned to a node determines its membership in a motif. For more comprehensive information regarding the datasets, please refer to Appendix A.1.

Methods: The methods used in this benchmarking are delineated in the green branch at Figure 1.

Metrics: We use the following metrics in our study:

- **Size:** In factual explanations, size denotes the number of edges in the explanation. In counterfactual, size denotes the number of edges perturbed to flip the label. Regardless of the explanation type, it is desirable for the explanation to be small.
- **Sufficiency (Fidelity):** Sufficiency encodes the ratio of graphs for which the prediction derived from the explanation matches the prediction obtained from the complete graph [43]. Its value spans between 0 and 1. For factual explanations, higher values indicate superior performance, while in counter-factual lower is better since the objective is to flip the class label. Some works have used the term *fidelity* instead of sufficiency. In addition, some papers have reported *necessity* which is simply 1-sufficiency/fidelity.

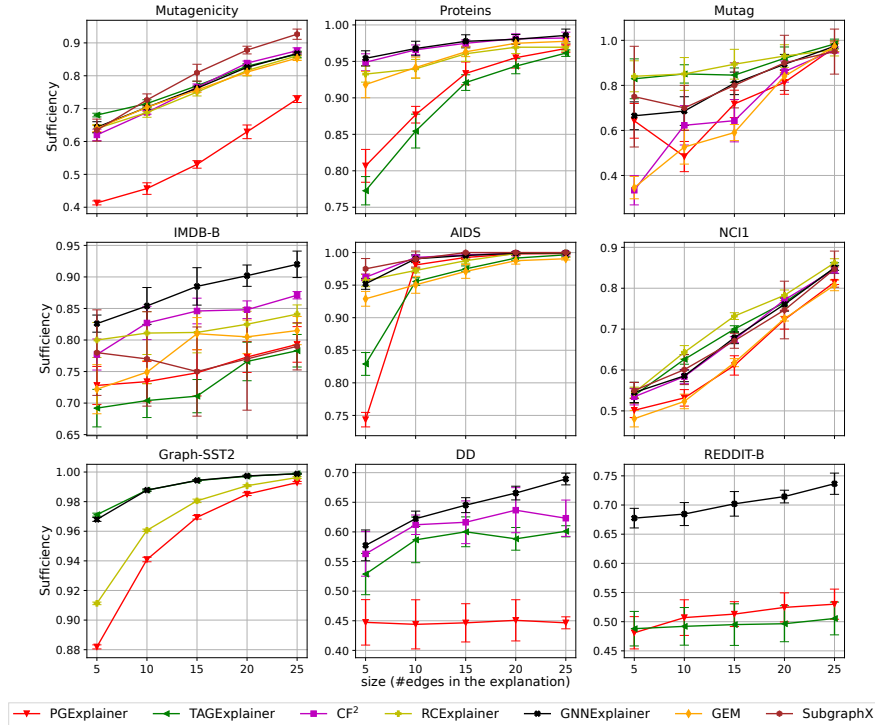


Figure 2: Sufficiency of the factual explainers against the explanation size. For factual explanations, higher is better. We omit those methods for a dataset that threw an out of memory (OOM) error.

- **Accuracy:** Accuracy represents the percentage of correct explanations. Computing accuracy is feasible only when ground-truth explanations are available, which in our case restricts us to node classification in the three datasets of TREE-CYCLES, TREE-GRID, and BA-SHAPES. In line with the standards set by CF^2 , CF -GNNEXPLAINER, and GEM, this metric pertains to the percentage of edges within the counterfactual that belong to the motif which decides the class.

4.1 Comparative Analysis

Factual Explainers: Fig. 2 illustrates the sufficiency analysis of various factual reasoners in relation to size. Each algorithm assigns a score to edges, indicating their likelihood of being included in the factual explanation. To control the size, we adopt a greedy approach by selecting the highest-scoring edges. Both CF^2 and RCEXPLAINER necessitate a parameter to balance factual and counterfactual explanations. We set this parameter to 1, corresponding to solely factual explanations.

Across the majority of datasets, PGEXPLAINER consistently delivers inferior results compared to other baseline methods. This behavior is more prominently visible in the spiderplot of the same data (See Fig. N in Appendix). However, it is challenging to identify a definitive best factual explainer, as no single technique dominates across all datasets. For instance, while RCEXPLAINER performs exceptionally well in the MUTAG dataset, it exhibits subpar performance in IMDB-B and GRAPH-SST2. Similar observations are also made for GNNEXPLAINER in REDDIT-B vs. MUTAG and NCI1. Overall, we recommend using either RCEXPLAINER or GNNEXPLAINER as the preferred choices. The spider plot in Fig. N more prominently substantiates this suggestion.

In Fig. 2, the sufficiency does not always increase monotonically with explanation size (such as PGEXPLAINER in Mutag). This behavior arises due to the combinatorial nature of the problem. Specifically, the impact of adding an edge to an existing explanation on the GNN prediction is a function of both the edge being added and the edges already included in the explanation. An explainer seeks to learn a proxy function that mimics the true combinatorial output of a set of edges. When this proxy function fails to predict the marginal impact of adding an edge, it could potentially select an edge that exerts a detrimental influence on the explanation’s quality.

Counterfactual Explainers: We present separate analyses for explanations generated over graph classification and node classification tasks.

Table 4 presents the results on graph classification. RCEXPLAINER is the best-performing explainer across majority of the datasets and metrics. However, it is important to acknowledge that RCEXPLAINER’s sufficiency, when objectively evaluated, consistently remains high which is undesired. For

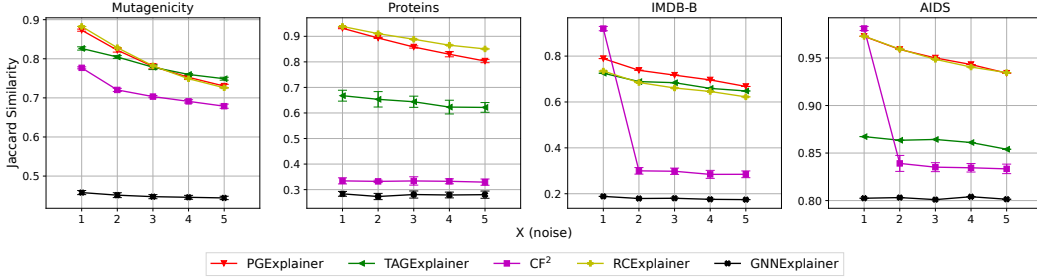


Figure 3: Stability of factual explainers in terms of Jaccard similarity of explanations against topological noise.

Table 4: Sufficiency and size of counterfactual explainers on graph classification. Lower values are better for both metrics. CF-GNNEXPLAINER is omitted since it is limited to node classification only. OOM indicates that the technique ran out of memory.

	Mutag		Mutagenicity		AIDS		Proteins		IMDB-B		ogbg-molhiv	
Method / Metric	Sufficiency↓	Size↓	Sufficiency↓	Size↓	Sufficiency↓	Size↓	Sufficiency↓	Size↓	Sufficiency↓	Size↓	Sufficiency↓	Size↓
RCEExplainer ($\lambda = 0$)	0.4 \pm 0.12	1.1 \pm 0.22	0.4 \pm 0.06	1.01 \pm 0.19	0.91 \pm 0.04	1.0 \pm 0.0	0.96 \pm 0.02	1.0 \pm 0.0	0.72 \pm 0.11	1.0 \pm 0.0	0.90 \pm 0.02	1 \pm 0.0
CF ² ($\alpha = 0$)	0.90 \pm 0.12	1.0 \pm 0.0	0.50 \pm 0.05	2.78 \pm 0.98	0.98 \pm 0.02	5.25 \pm 0.35	1.0 \pm 0.0	NA	0.81 \pm 0.07	8.57 \pm 4.99	0.96 \pm 0.00	10.45 \pm 4.43
CLEAR	0.55 \pm 0.1	17.15 \pm 1.62	OOM	OOM	0.84 \pm 0.03	164.95 \pm 47.93	OOM	OOM	0.96 \pm 0.02	218.62 \pm 0.0	OOM	OOM

instance, in the case of AIDS, the sufficiency of RCEXPLAINER reaches a value of 0.9, signifying its inability to generate counterfactual explanations for 90% of the graphs. This observation suggests that there exists considerable potential for further enhancement. We also note that while CLEAR achieves the best (lowest) sufficiency in AIDS, the number of perturbations it requires (size) is exorbitantly high to be useful in practical use-cases.

Table 5 presents the results on node classification. We observe that CF-GNNEXPLAINER consistently outperforms CF² ($\alpha = 0$ indicates the method to be entirely counterfactual). We note that our result contrasts with the reported results in CF² [43], where CF² was shown to outperform CF-GNNEXPLAINER. Finally, when compared to graph classification, the sufficiency produced by the best methods in the node classification task is significantly lower indicating that it is an easier task. One possible reason might be the space of counterfactuals is smaller in node classification.

4.2 Stability

We next examine the stability of the explanations against topological noise, model parameters, and the choice of GNN architecture. Given a graph $\mathcal{G}(\mathcal{V}, \mathcal{E})$, let $\mathcal{E}_X \subset \mathcal{E}$ and $\mathcal{E}'_X \subseteq \mathcal{E}$ be the set of edges in the original and perturbed explanations respectively. We measure stability by computing the *Jaccard similarity* between the two sets, i.e., $\frac{|\mathcal{E}_X \cap \mathcal{E}'_X|}{|\mathcal{E}_X \cup \mathcal{E}'_X|}$. In App. B, we present the impact of the above mentioned factors on other metrics of interest such as sufficiency and explanation size. In addition, we also present impact of feature perturbation and topological adversarial attack in App. B.

Factual-stability against topological noise: Fig. 3 illustrates the Jaccard coefficient as a function of the noise volume. Similar to Fig. 2, edge selection for the explanation involves a greedy approach that prioritizes the highest score edges. RCEXPLAINER (executed at $\alpha = 1$) and PGEXPLAINER consistently exhibit higher stability. This consistent performance reinforces the claim that RCEXPLAINER is the preferred factual explainer. The stability of RCEXPLAINER can be attributed to its strategy of selecting a subset of edges that is resistant to changes, such that the removal of these edges significantly impacts the prediction made by the remaining graph [6]. PGEXPLAINER also incorporates a form of inherent stability within its framework. It builds upon the concept introduced in GNNEXPLAINER through the assumption that the explanatory graph can be modeled as a random Gilbert graph, where the probability distribution of edges is conditionally independent and can be parameterized. This generic assumption holds the potential to enhance the stability of the method. Conversely, TAGEXPLAINER exhibits the lower stability than RCEXPLAINER and PGEXPLAINER, likely due to its reliance solely on gradients in a task-agnostic manner [51]. The exclusive reliance on gradients makes it more susceptible to overfitting, resulting in reduced stability.

Factual-Stability against explainer instances: Table 6 presents the stability of explanations provided across three different explainer instances on the same black-box GNN. A similar trend is observed, with RCEXPLAINER remaining the most robust method, while GNNEXPLAINER exhibits the least stability. For GNNEXPLAINER, the Jaccard coefficient hovers around 0.5, indicating significant variance in explaining the same GNN. This lack of stability may hinder the practical adoption of factual explainers for real-world use cases.

Table 5: Performance of counterfactual explainers on node classification. Shaded cells indicate the best result in a column. Note that only CF-GNNEXPLAINER and CF² can explain node classification.

Method / Metric	Tree-Cycles			Tree-Grid			BA-Shapes		
	Sufficiency ↓	Size ↓	Acc.(%) ↑	Sufficiency ↓	Size ↓	Acc.(%) ↑	Sufficiency ↓	Size ↓	Acc.(%) ↑
CF-GNNEXPLAINER	0.5 ±0.08	1.03 ±0.16	100.0 ±0.0	0.09 ±0.06	1.42 ±0.55	92.70 ±4.99	0.37 ±0.05	1.37 ±0.59	91.5 ±4.36
CF ² (α=0)	0.76 ±0.06	4.55 ±1.48	74.71 ±18.70	0.99 ±0.02	7.0 ±0.0	14.29 ±0.0	0.25 ±0.88	4.24 ±1.70	68.89 ±12.28

Table 6: Stability in explanations provided by factual explainers across runs. We fix the size to 10 for all explainers. The most stable explainer for each dataset (row) corresponding to the three categories of 1vs2, 1vs3 and 2vs3 are highlighted through gray, yellow and cyan shading respectively.

Dataset / Seeds	PGExplainer			TAGExplainer			CF ²			RCExplainer			GNNExplainer		
	1vs2	1vs3	2vs3	1vs2	1vs3	2vs3	1vs2	1vs3	2vs3	1vs2	1vs3	2vs3	1vs2	1vs3	2vs3
Mutagenicity	0.69	0.75	0.62	0.76	0.78	0.74	0.77	0.77	0.77	0.75	0.71	0.71	0.46	0.47	0.47
Proteins	0.38	0.51	0.38	0.55	0.48	0.46	0.34	0.34	0.35	0.88	0.85	0.91	0.28	0.28	0.28
Mutag	0.5	0.54	0.51	0.36	0.43	0.72	0.78	0.79	0.79	0.86	0.92	0.87	0.57	0.57	0.58
IMDB-B	0.67	0.76	0.67	0.67	0.60	0.56	0.32	0.32	0.32	0.75	0.73	0.70	0.18	0.19	0.18
AIDS	0.88	0.87	0.82	0.81	0.83	0.87	0.85	0.85	0.85	0.95	0.96	0.97	0.80	0.80	0.80
NCI1	0.58	0.55	0.64	0.69	0.81	0.65	0.60	0.60	0.60	0.71	0.71	0.94	0.44	0.44	0.44

Factual-Stability against GNN architectures: Finally, we explore the stability of explainers across different GNN architectures in Table 7, which has not yet been investigated in the existing literature. For each combination of architectures, we assess the stability by computing the Jaccard coefficient between the explained predictions of the indicated GNN architecture and the default GCN model. One notable finding is that the stability of explainers exhibits a strong correlation with the dataset used. Specifically, in five out of six datasets, the best performing explainer across all architectures is unique. However, it is important to highlight that the Jaccard coefficients across architectures consistently remain low indicating stability against different architectures is the hardest objective due to the variations in their message aggregating schemes.

Stability of counterfactual explainers: Table 8 provides an overview of the stability exhibited among explainer instances trained using three distinct seeds. Notably, we observe a substantial Jaccard index,

Table 8: Stability against explainer instances. Note that stability wrt a graph is computable only if both explainer instances find its counterfactual. “NA” indicates scenarios when no such graph exists in the test set.

Dataset / Seeds	RCExplainer			CF ²			CLEAR		
	1vs2	1vs3	2vs3	1vs2	1vs3	2vs3	1vs2	1vs3	2vs3
Mutagenicity	0.96 ±0.06	0.96 ±0.04	0.98 ±0.03	0.90 ±0.09	0.89 ±0.1	0.89 ±0.11	OOM	OOM	OOM
Proteins	0.95 ±0.0	0.94 ±0.0	0.90 ±0.0	NA	NA	NA	OOM	OOM	OOM
Mutag	0.98 ±0.03	0.98 ±0.03	1.0 ±0.0	1.0 ±0.0	1.0 ±0.0	1.0 ±0.0	0.55 ±0.01	0.53 ±0.01	0.54 ±0.02
IMDB-B	0.99 ±0.01	1.0 ±0.0	0.99 ±0.01	0.96 ±0.05	0.95 ±0.06	0.94 ±0.07	0.28 ±0.0	0.27 ±0.0	0.28 ±0.0
AIDS	0.84 ±0.04	0.96 ±0.06	0.84 ±0.04	NA	1.0 ±0.0	NA	0.19 ±0.02	0.20 ±0.03	0.19 ±0.04
ogbg-molhiv	0.99 ±0.03	0.99 ±0.04	0.99 ±0.04	0.801 ±0.149	0.764 ±0.14	0.784 ±0.144	OOM	OOM	OOM

indicating favorable stability, in the case of RCExplainer and CF² explainers. Conversely, CLEAR fails to demonstrate comparable stability. These findings align with the outcomes derived from Table 4. Specifically, when RCExplainer and CF² are successful in identifying a counterfactual, the resultant counterfactual graphs are obtained through a small number of perturbations. Consequently, the counterfactual graphs exhibit similarities to the original graph, rendering them akin to one another. However, this trend does not hold true for CLEAR, as it necessitates a significantly greater number of perturbations.

Similar observations are made concerning stability in the presence of topological noise and various GNN architectures, owing to the aforementioned reasons. For detailed results, please refer to App. B.

4.3 Necessity and Reproducibility

Recall the definitions of necessity and sufficiency from § 3. In both cases, we evaluate performance using sufficiency as the metric. Sufficiency, in this context, measures the ratio of graphs for which the GNN prediction on the residual graph is the same as in the original graph. Following the removal of explanation, we expect sufficiency to be low.

The results are presented in the form of plots in App. C (due to space limitations). While sufficiency is indeed low in necessity, this is not the case in reproducibility. These findings suggest that while current factual explainers effectively explain the model, they do not provide a comprehensive explanation of the underlying data. The fact that the GNN can regain prediction accuracy when retrained indicates the presence of other signals that the initial factual explanation failed to capture.

4.4 Feasibility

Counterfactual explanations serve as recourses and are expected to generate graphs that adhere to the feasibility constraints of the pertinent domain. Given that the benchmarked algorithms are

Table 7: Stability of factual explainers against the GNN architecture. We fix the size to 10. We report the Jaccard coefficient of explanations obtained for each architecture against the explanation provided over GCN. The best explainers for each dataset (row) are highlighted in gray, yellow and cyan shading for GAT, GIN, and GRAPHSAGE, respectively. GRAPHSAGE is denoted by SAGE.

Dataset / Architecture	PGExplainer			TAGExplainer			CF ²			RCExplainer			GNNExplainer		
	GAT	GIN	SAGE	GAT	GIN	SAGE	GAT	GIN	SAGE	GAT	GIN	SAGE	GAT	GIN	SAGE
Mutagenicity	0.63	0.65	0.60	0.24	0.25	0.32	0.52	0.47	0.54	0.56	0.52	0.46	0.43	0.42	0.43
Proteins	0.22	0.47	0.38	0.45	0.41	0.18	0.28	0.28	0.28	0.37	0.41	0.42	0.28	0.28	0.28
Mutag	0.57	0.58	0.69	0.60	0.65	0.64	0.58	0.56	0.62	0.47	0.76	0.54	0.55	0.57	0.55
IMDB-B	0.48	0.45	0.56	0.44	0.35	0.47	0.17	0.23	0.17	0.30	0.33	0.26	0.17	0.17	0.17
AIDS	0.81	0.85	0.87	0.83	0.83	0.84	0.80	0.80	0.80	0.81	0.85	0.81	0.8	0.8	0.8
NCI1	0.39	0.41	0.37	0.45	0.17	0.58	0.37	0.38	0.38	0.49	0.53	0.52	0.37	0.38	0.39

agnostic to specific domains, our initial evaluation entails examining whether these algorithms preserve the topological properties of the test set. To achieve this, we compare the number of graphs forming a single connected component in the test set with those in their corresponding counterfactual explanations. Connectedness is a significant aspect of consideration, particularly in domains such as molecules, where disconnected graphs are rare occurrences and might not be meaningful. The results for RCExplainer are presented in Table 9.

We use RCExplainer for this experiment since it is the most robust and well-performing algorithm among those we have benchmarked. Notably, we observe statistically significant deviations from the expected values in two out of four molecular datasets. This suggests a heightened probability of predicting counterfactuals that do not correspond to feasible molecules. Importantly, this finding underscores a limitation of counterfactual explainers, which has received limited attention within the research community.

Table 9: **Feasibility:** Assessing the statistical significance of deviations in the number of connected graphs between the test set and their corresponding counterfactual explanations on molecular datasets. Statistically significant deviations with p -value < 0.05 are highlighted.

Dataset	Expected Count	Observed Count	p -value
Mutagenicity	233.05	70	< 0.00001
Proteins	11.68	12	0.93
Mutag	11.0	9.0	0.55
AIDS	17.6	8	0.02

4.5 Visualization-based Analysis

We include visualization based analysis of the explanations in App. D. Due to space limitations, we omit the details here. Our analysis reveal that a statistically good performance do not always align with human judgement indicating an urgent need for datasets annotated with ground truth explanations. Furthermore, the visualization analysis reinforces the need to incorporate feasibility as desirable component in counterfactual reasoning.

5 Concluding Insights

Our benchmarking study has yielded several insights that can streamline the development of explanation algorithms. We summarize the key findings below.

- **Performance and Stability:** Among the explainers evaluated, RCExplainer consistently outperformed others in terms of efficacy and stability to noise and variational factors (§ 4.1 and § 4.2).
- **Stability Concerns:** Most factual explainers demonstrated significant deviations across explainer instances, vulnerability to topological perturbations and produced significantly different set of explanations across different GNN architectures. These stability notions should therefore be embraced as desirable factors along with other performance metrics.
- **Model Explanation vs. Data Explanation:** Our experiments on reproducibility (§ 4.3) revealed that even without the factual explanation, the GNN model predicted accurately on the residual graph. This suggests that explainers only capture specific signals learned by the GNN and do not encompass all underlying data signals.
- **Feasibility Issues:** Counterfactual explanations showed deviations in topological distribution from the original graphs, raising feasibility concerns (§ 4.4).

We hope that the aforementioned insights would offer new directions for advancing GNN explainers, allowing researchers to address limitations and enhance the overall quality and interpretability of GNNs.

Limitations. Our study only focuses on perturbation-based instance-specific methods. We hope to replicate the same study on the branches shown in Fig. 1.

References

- [1] Carlo Abrate and Francesco Bonchi. Counterfactual graphs for explainable classification of brain networks. In *KDD*, page 2495–2504, 2021.
- [2] Chirag Agarwal, Owen Queen, Himabindu Lakkaraju, and Marinka Zitnik. Evaluating explainability for graph neural networks. 2023.
- [3] Miltiadis Allamanis, Earl T Barr, Premkumar Devanbu, and Charles Sutton. A survey of machine learning for big code and naturalness. *ACM Computing Surveys (CSUR)*, 51(4):1–37, 2018.
- [4] Kenza Amara, Zhitao Ying, Zitao Zhang, Zhichao Han, Yang Zhao, Yinan Shan, Ulrik Brandes, Sebastian Schemm, and Ce Zhang. Graphframex: Towards systematic evaluation of explainability methods for graph neural networks. In *The First Learning on Graphs Conference*, 2022.
- [5] Steve Azzolin, Antonio Longa, Pietro Barbiero, Pietro Lio, and Andrea Passerini. Global explainability of GNNs via logic combination of learned concepts. In *The Eleventh International Conference on Learning Representations*, 2023.
- [6] Mohit Bajaj, Lingyang Chu, Zi Yu Xue, Jian Pei, Lanjun Wang, Peter Cho-Ho Lam, and Yong Zhang. Robust counterfactual explanations on graph neural networks. In A. Beygelzimer, Y. Dauphin, P. Liang, and J. Wortman Vaughan, editors, *Advances in Neural Information Processing Systems*, 2021.
- [7] Federico Baldassarre and Hossein Azizpour. Explainability techniques for graph convolutional networks. *arXiv preprint arXiv:1905.13686*, 2019.
- [8] Ravinder Bhattoo, Sayan Ranu, and NM Krishnan. Learning articulated rigid body dynamics with lagrangian graph neural network. *Advances in Neural Information Processing Systems*, 35:29789–29800, 2022.
- [9] Ravinder Bhattoo, Sayan Ranu, and NM Anoop Krishnan. Learning the dynamics of particle-based systems with lagrangian graph neural networks. *Machine Learning: Science and Technology*, 2023.
- [10] Suresh Bishnoi, Ravinder Bhattoo, Sayan Ranu, and NM Krishnan. Enhancing the inductive biases of graph neural ode for modeling dynamical systems. *ICLR*, 2023.
- [11] Karsten M Borgwardt, Cheng Soon Ong, Stefan Schöner, SVN Vishwanathan, Alex J Smola, and Hans-Peter Kriegel. Protein function prediction via graph kernels. *Bioinformatics*, 21(suppl_1):i47–i56, 2005.
- [12] Yuwei Cao, Hao Peng, Jia Wu, Yingdong Dou, Jianxin Li, and Philip S Yu. Knowledge-preserving incremental social event detection via heterogeneous gnns. In *Proceedings of the Web Conference 2021*, pages 3383–3395, 2021.
- [13] Pritish Chakraborty, Sayan Ranu, Krishna Sri Ipsit Mantri, and Abir De. Learning and maximizing influence in social networks under capacity constraints. In *Proceedings of the Sixteenth ACM International Conference on Web Search and Data Mining*, pages 733–741, 2023.
- [14] Asim Kumar Debnath, Rosa L Lopez de Compadre, Gargi Debnath, Alan J Shusterman, and Corwin Hansch. Structure-activity relationship of mutagenic aromatic and heteroaromatic nitro compounds. correlation with molecular orbital energies and hydrophobicity. *Journal of medicinal chemistry*, 34(2):786–797, 1991.
- [15] Paul D Dobson and Andrew J Doig. Distinguishing enzyme structures from non-enzymes without alignments. *Journal of molecular biology*, 330(4):771–783, 2003.
- [16] Gérard Hamiache and Florian Navarro. Associated consistency, value and graphs. *International Journal of Game Theory*, 49:227–249, 2020.
- [17] William L. Hamilton, Rex Ying, and Jure Leskovec. Inductive representation learning on large graphs. In *Proceedings of the 31st International Conference on Neural Information Processing Systems, NIPS’17*, page 1025–1035, Red Hook, NY, USA, 2017. Curran Associates Inc.
- [18] Qiang Huang, Makoto Yamada, Yuan Tian, Dinesh Singh, and Yi Chang. Graphlime: Local interpretable model explanations for graph neural networks. *IEEE Transactions on Knowledge and Data Engineering*, 2022.

- [19] Zexi Huang, Mert Kosan, Sourav Medya, Sayan Ranu, and Ambuj Singh. Global counterfactual explainer for graph neural networks. In *Proceedings of the Sixteenth ACM International Conference on Web Search and Data Mining*, pages 141–149, 2023.
- [20] Sergei Ivanov, Sergei Sviridov, and Evgeny Burnaev. Understanding isomorphism bias in graph data sets. *Geometric Learning and Graph Representations ICLR Workshop*, 2019.
- [21] Mingjian Jiang, Zhen Li, Shugang Zhang, Shuang Wang, Xiaofeng Wang, Qing Yuan, and Zhiqiang Wei. Drug–target affinity prediction using graph neural network and contact maps. *RSC advances*, 10(35):20701–20712, 2020.
- [22] Jaykumar Kakkad, Jaspal Jannu, Kartik Sharma, Charu Aggarwal, and Sourav Medya. A survey on explainability of graph neural networks. *arXiv preprint arXiv:2306.01958*, 2023.
- [23] Jeroen Kazius, Ross McGuire, and Roberta Bursi. Derivation and validation of toxicophores for mutagenicity prediction. *Journal of medicinal chemistry*, 48(1):312–320, 2005.
- [24] Thomas N Kipf and Max Welling. Semi-supervised classification with graph convolutional networks. *arXiv preprint arXiv:1609.02907*, 2016.
- [25] Mert Kosan, Arlei Silva, Sourav Medya, Brian Uzzi, and Ambuj Singh. Event detection on dynamic graphs. *arXiv preprint arXiv:2110.12148*, 2021.
- [26] Mert Kosan, Arlei Silva, and Ambuj Singh. Robust ante-hoc graph explainer using bilevel optimization. *arXiv preprint arXiv:2305.15745*, 2023.
- [27] Wanyu Lin, Hao Lan, and Baochun Li. Generative causal explanations for graph neural networks. In *International Conference on Machine Learning*, pages 6666–6679. PMLR, 2021.
- [28] Wanyu Lin, Hao Lan, and Baochun Li. Generative causal explanations for graph neural networks. In *ICML*, 2021.
- [29] Ana Lucic, Maartje A Ter Hoeve, Gabriele Tolomei, Maarten De Rijke, and Fabrizio Silvestri. Cf-gnnexplainer: Counterfactual explanations for graph neural networks. In *AISTATS*, pages 4499–4511, 2022.
- [30] Dongsheng Luo, Wei Cheng, Dongkuan Xu, Wenchao Yu, Bo Zong, Haifeng Chen, and Xiang Zhang. Parameterized explainer for graph neural network. *Advances in neural information processing systems*, 33:19620–19631, 2020.
- [31] Jing Ma, Ruocheng Guo, Saumitra Mishra, Aidong Zhang, and Jundong Li. Clear: Generative counterfactual explanations on graphs. *arXiv preprint arXiv:2210.08443*, 2022.
- [32] Sahil Manchanda, Akash Mittal, Anuj Dhawan, Sourav Medya, Sayan Ranu, and Ambuj Singh. Gcomb: Learning budget-constrained combinatorial algorithms over billion-sized graphs. *Advances in Neural Information Processing Systems*, 33:20000–20011, 2020.
- [33] Phillip E Pope, Soheil Kolouri, Mohammad Rostami, Charles E Martin, and Heiko Hoffmann. Explainability methods for graph convolutional neural networks. In *Proceedings of the IEEE/CVF conference on computer vision and pattern recognition*, pages 10772–10781, 2019.
- [34] Mario Alfonso Prado-Romero, Bardh Prenkaj, Giovanni Stilo, and Fosca Giannotti. A survey on graph counterfactual explanations: Definitions, methods, evaluation, and research challenges. *ACM Computing Surveys*, 2023.
- [35] Ladislav Rampášek, Mikhail Galkin, Vijay Prakash Dwivedi, Anh Tuan Luu, Guy Wolf, and Dominique Beaini. Recipe for a General, Powerful, Scalable Graph Transformer. *Advances in Neural Information Processing Systems*, 35, 2022.
- [36] Rishabh Ranjan, Siddharth Grover, Sourav Medya, Venkatesan Chakaravarthy, Yogish Sabharwal, and Sayan Ranu. Greed: A neural framework for learning graph distance functions. In *Advances in Neural Information Processing Systems*, 2022.
- [37] Kaspar Riesen and Horst Bunke. Iam graph database repository for graph based pattern recognition and machine learning. In *Joint IAPR International Workshops on Statistical Techniques in Pattern Recognition (SPR) and Structural and Syntactic Pattern Recognition (SSPR)*, pages 287–297. Springer, 2008.
- [38] Thomas Schnake, Oliver Eberle, Jonas Lederer, Shinichi Nakajima, Kristof T Schütt, Klaus-Robert Müller, and Grégoire Montavon. Higher-order explanations of graph neural networks via relevant walks. *IEEE transactions on pattern analysis and machine intelligence*, 44(11):7581–7596, 2021.

- [39] Robert Schwarzenberg, Marc Hübner, David Harbecke, Christoph Alt, and Leonhard Henning. Layerwise relevance visualization in convolutional text graph classifiers. *arXiv preprint arXiv:1909.10911*, 2019.
- [40] Caihua Shan, Yifei Shen, Yao Zhang, Xiang Li, and Dongsheng Li. Reinforcement learning enhanced explainer for graph neural networks. In *NeurIPS 2021*, December 2021.
- [41] Lloyd S Shapley et al. A value for n-person games. 1953.
- [42] Richard Socher, A. Perelygin, J.Y. Wu, J. Chuang, C.D. Manning, A.Y. Ng, and C. Potts. Recursive deep models for semantic compositionality over a sentiment treebank. *EMNLP*, 1631:1631–1642, 01 2013.
- [43] Juntao Tan, Shijie Geng, Zuohui Fu, Yingqiang Ge, Shuyuan Xu, Yunqi Li, and Yongfeng Zhang. Learning and evaluating graph neural network explanations based on counterfactual and factual reasoning. In *Proceedings of the ACM Web Conference 2022*, WWW ’22, page 1018–1027, 2022.
- [44] Abishek Thangamuthu, Gunjan Kumar, Suresh Bishnoi, Ravinder Bhattoo, NM Krishnan, and Sayan Ranu. Unravelling the performance of physics-informed graph neural networks for dynamical systems. In *Advances in Neural Information Processing Systems*, 2022.
- [45] Petar Veličković, Guillem Cucurull, Arantxa Casanova, Adriana Romero, Pietro Liò, and Yoshua Bengio. Graph attention networks. In *International Conference on Learning Representations*, 2018.
- [46] Paul Voigt and Axel Von dem Bussche. The eu general data protection regulation (gdpr). *A Practical Guide, 1st Ed.*, Cham: Springer International Publishing, 10(3152676):10–5555, 2017.
- [47] Minh Vu and My T Thai. Pgm-explainer: Probabilistic graphical model explanations for graph neural networks. *Advances in neural information processing systems*, 33:12225–12235, 2020.
- [48] Nikil Wale, Ian A Watson, and George Karypis. Comparison of descriptor spaces for chemical compound retrieval and classification. *Knowledge and Information Systems*, 14(3):347–375, 2008.
- [49] Xingchen Wan, Henry Kenlay, Binxin Ru, Arno Blaas, Michael Osborne, and Xiaowen Dong. Adversarial attacks on graph classifiers via bayesian optimisation. In *Thirty-Fifth Conference on Neural Information Processing Systems*, 2021.
- [50] Geemi P Wellawatte, Aditi Seshadri, and Andrew D White. Model agnostic generation of counterfactual explanations for molecules. *Chemical science*, 13(13):3697–3705, 2022.
- [51] Yaochen Xie, Sumeet Katariya, Xianfeng Tang, Edward Huang, Nikhil Rao, Karthik Subbian, and Shuiwang Ji. Task-agnostic graph explanations. *NeurIPS*, 2022.
- [52] Jiacheng Xiong, Zhaoping Xiong, Kaixian Chen, Hualiang Jiang, and Mingyue Zheng. Graph neural networks for automated de novo drug design. *Drug Discovery Today*, 26(6):1382–1393, 2021.
- [53] Keyulu Xu, Weihua Hu, Jure Leskovec, and Stefanie Jegelka. How powerful are graph neural networks? In *International Conference on Learning Representations*, 2019.
- [54] Han Xuanyuan, Pietro Barbiero, Dobrik Georgiev, Lucie Charlotte Magister, and Pietro Lió. Global concept-based interpretability for graph neural networks via neuron analysis. 2023.
- [55] Pinar Yanardag and SVN Vishwanathan. Deep graph kernels. In *Proceedings of the 21th ACM SIGKDD international conference on knowledge discovery and data mining*, pages 1365–1374, 2015.
- [56] Chengxuan Ying, Tianle Cai, Shengjie Luo, Shuxin Zheng, Guolin Ke, Di He, Yanming Shen, and Tie-Yan Liu. Do transformers really perform badly for graph representation? In A. Beygelzimer, Y. Dauphin, P. Liang, and J. Wortman Vaughan, editors, *Advances in Neural Information Processing Systems*, 2021.
- [57] Rex Ying, Dylan Bourgeois, Jiaxuan You, Marinka Zitnik, and Jure Leskovec. Gnnexplainer: Generating explanations for graph neural networks. *Advances in neural information processing systems*, 32:9240, 2019.

- [58] Rex Ying, Ruining He, Kaifeng Chen, Pong Eksombatchai, William L. Hamilton, and Jure Leskovec. Graph convolutional neural networks for web-scale recommender systems. In *KDD*, page 974–983, 2018.
- [59] Zhitao Ying, Dylan Bourgeois, Jiaxuan You, Marinka Zitnik, and Jure Leskovec. Gnnexplainer: Generating explanations for graph neural networks. *Advances in neural information processing systems*, 32, 2019.
- [60] Hao Yuan, Jiliang Tang, Xia Hu, and Shuiwang Ji. Xggn: Towards model-level explanations of graph neural networks. In *Proceedings of the 26th ACM SIGKDD International Conference on Knowledge Discovery & Data Mining*, pages 430–438, 2020.
- [61] Hao Yuan, Haiyang Yu, Shurui Gui, and Shuiwang Ji. Explainability in graph neural networks: A taxonomic survey. *IEEE Transactions on Pattern Analysis and Machine Intelligence*, 2022.
- [62] Hao Yuan, Haiyang Yu, Jie Wang, Kang Li, and Shuiwang Ji. On explainability of graph neural networks via subgraph explorations. In *ICML*, pages 12241–12252. PMLR, 2021.
- [63] Shichang Zhang, Yozen Liu, Neil Shah, and Yizhou Sun. Gstarx: Explaining graph neural networks with structure-aware cooperative games. In *Advances in Neural Information Processing Systems*, 2022.
- [64] Yue Zhang, David Defazio, and Arti Ramesh. Relex: A model-agnostic relational model explainer. In *Proceedings of the 2021 AAAI/ACM Conference on AI, Ethics, and Society*, pages 1042–1049, 2021.

Appendix

A Experimental Setup

All experiments were conducted using the Ubuntu 18.04 operating system on an NVIDIA DGX Station equipped with four V100 GPU cards, each having 128GB of GPU memory. The system also included 256GB of RAM and a 20-core Intel Xeon E5-2698 v4 2.2 GHz CPU.

The datasets for factual and counterfactual explainers follow an 80:10:10 split for training, validation and testing. We explain some of our design choices below.

- For factual explainers, the inductive explainers are trained on the training data and the reported results are computed on the entire dataset. We also report results only on test data (please see Sec. A.2) comparing only inductive methods. Transductive methods are run on the entire dataset.
- For counterfactual explainers, the inductive explainers are trained on the training data, and the reported results are computed on the test data. Since transductive methods do not have the notion of training and testing separately, they are run only on the test data.

A.1 Benchmark Datasets

Datasets for Node classification: The following datasets have node labels and are used for the node classification task.

- **TREE-CYCLES [59]:** The base graph used in this dataset is a binary tree, and the motifs consist of **6-node cycles** (Figure D(a)). The motifs are connected to random nodes in the tree. Non-motif nodes are labeled 0, while the motif nodes are labeled 1.
- **TREE-GRID [59]:** The base graph used in this dataset is a binary tree, and the motif is a **3 × 3 grid** connected to random nodes in the tree (Figure D(b)). Similar to the tree-cycles dataset, the nodes are labeled with binary classes (0 for the non-motif nodes and 1 for the motif nodes).
- **BA-SHAPES [59]:** The base graph in this dataset is a Barabasi-Albert (BA) graph. The dataset includes **house-shaped** structures composed of 5 nodes (Figure D (c)). Non-motif nodes are assigned class 0, while nodes at the top, middle, and bottom of the motif are assigned classes 1, 2, and 3, respectively.

Datasets for Graph Classification: The following datasets are used for the graph classification task and contain labeled graphs.

- **MUTAG [20] and Mutagenicity [37, 23]:** These are graph datasets containing chemical compounds. The nodes represent atoms, and the edges represent chemical bonds. The binary labels depend on the mutagenic effect of the compound on a bacterium, namely mutagenic or non-mutagenic. MUTAG and Mutagenicity datasets contain 188 and 4337 graphs, respectively.
- **AIDS: [20]** This dataset contains small molecules. The nodes and edges are atoms and chemical bonds, respectively. The molecules are classified by whether they are active against the HIV virus or not.
- **Proteins [11, 15] and DD [15]:** These datasets are comprised of proteins categorized into enzymes and non-enzymes. The nodes represent amino acids, and an edge exists between two nodes if their distance is less than 6 Angstroms.
- **NCII [48]:** This dataset is derived from cheminformatics and represents chemical compounds as input graphs. Vertices in the graph correspond to atoms, while edges represent bonds between atoms. This dataset focuses on anti-cancer screenings for cell lung cancer, with chemicals labeled as positive or negative. Each vertex is assigned an input label indicating the atom type, encoded using a one-hot-encoding scheme.
- **IMDB-B [55]:** The IMDB-BINARY dataset is a collection of movie collaboration networks, encompassing the ego-networks of 1,000 actors and actresses who have portrayed roles in films listed on IMDB. Each network is represented as a graph, where the nodes correspond to the actors/actresses, and an edge is present between two nodes if they have shared the screen in the same movie. These graphs have been constructed specifically from movies in the Action and Romance genres, which are the class labels.
- **REDDIT-B [55]:** REDDIT-BINARY dataset encompasses graphs representing online discussions on Reddit. Each graph has nodes representing users, connected by edges when either user responds to the other’s comment. The four prominent subreddits within this dataset are IAmA, AskReddit,

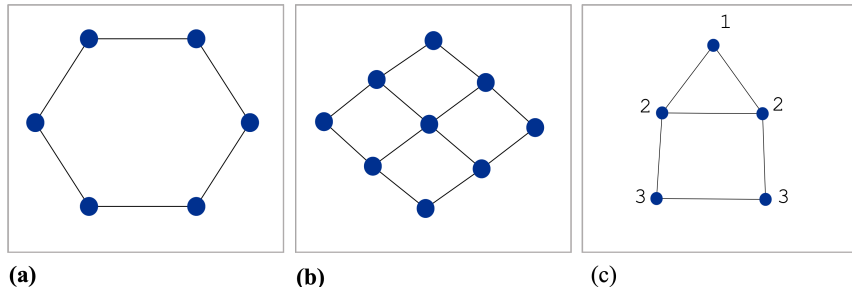


Figure D: Motifs used in (a) Tree-Cycles, (b) Tree-Grid and (c) BA-Shapes datasets for the node classification task. Please note the following. (i) Tree-Cycles and Tree-Grid have labels 0 and 1 for the non-motif and the motif nodes, respectively. Hence, all nodes in (a) and (b) have label 1. (ii) BA-Shapes dataset has 4 classes. Non-motif nodes have labels 0; motif nodes have integral labels depending on the position in the house motif. The other labels are 1 (top node), 2 (middle nodes) and 3 (bottom nodes). They are represented in (c).

TrollXChromosomes, and atheism. IAmA and AskReddit are question/answer-based communities, while TrollXChromosomes and atheism are discussion-based communities. Graphs are labeled based on their affiliation with either a question/answer-based or discussion-based community.

- **GRAPH-SST2 [61]:** The Graph-SST2 dataset is a graph-based dataset derived from the SST2 dataset [42], which contains movie review sentences labeled with positive or negative sentiment. Each sentence in the Graph-SST2 dataset is transformed into a graph representation, with words as nodes and edges representing syntactic relationships capturing the sentence’s grammatical structure. The sentiment labels from the original SST2 dataset are preserved, allowing for sentiment analysis tasks using the graph representations of the sentences.
- **ogbg-molhiv [3]:** ogbg-molhiv is a molecule dataset with nodes representing atoms and edges representing chemical bonds. The node features represent various properties of the atoms like chirality, atomic number, formal charge etc. Edge attributes represent the bond type. We study binary classification task on this dataset. The task is to achieve the most accurate predictions of specific molecular properties. These properties are framed as binary labels, indicating attributes like whether a molecule demonstrates inhibition of HIV virus replication or not.

A.2 Factual Explainers: Inductive Methods on Test Set

The inductive factual explainers are run only on the test data and the results are reported in Figure E. The results are similar to the ones where the methods are run on the entire dataset (Figure 2). Consistent with the earlier results, PGEXPLAINER consistently delivers inferior results compared to other baseline methods, and no single technique dominates across all datasets. Overall, RCEXPLAINER could be recommended as one of the preferred choices.

A.3 Details of GNN model Φ used for Node Classification

We use the same GNN model used in CF-GNNEXPLAINER and CF². Specifically, it is a Graph Convolutional Networks [24] trained on each of the datasets. Each model has 3 graph convolutional layers with 20 hidden dimensions for the benchmark datasets. The non-linearity used is *relu* for the first two layers and *log softmax* after the last layer of GCN. The learning rate is 0.01. The train and test data are divided in the ratio 80:20. The accuracy of the GNN model Φ for each dataset is mentioned in Table J.

A.4 Details of Base GNN Model Φ for the Graph Classification Task

Our GNN models have an optional parameter for continuous edge weights, which in our case represents explanations. Each model consists of 3 layers with 20 hidden dimensions specifically designed for benchmark datasets. The models provide node embeddings, graph embeddings, and direct outputs from the model (without any softmax function). The output is obtained through a one-layer MLP applied to the graph embedding. We utilize the max pooling operator to calculate the graph embedding. The dropout rate, learning rate, and batch size are set to 0, 0.001, and 128, respectively.

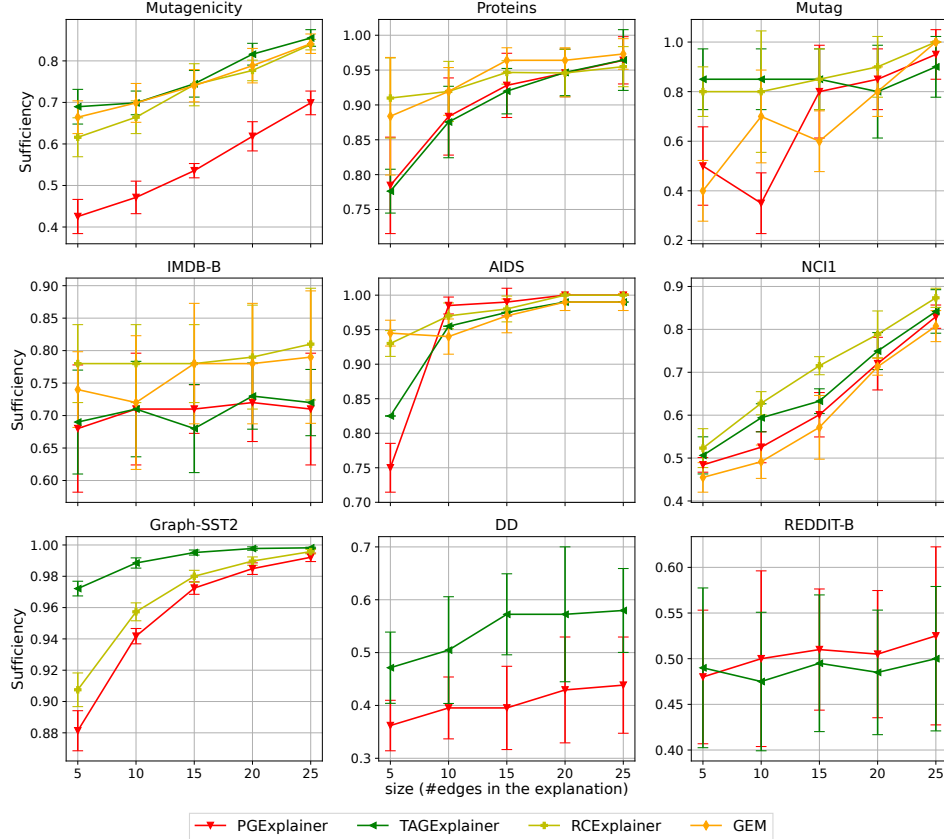


Figure E: Sufficiency of the inductive factual explainers against the explanation size on only test data. For factual explanations, higher is better. We omit those methods for a dataset that throw an out-of-memory (OOM) error and are not scalable.

Table J: Accuracy of black-box GNN Φ on the datasets used for node classification, for evaluation of counterfactual explainers. Φ is a GCN [24] for this task

Dataset	Train accuracy	Test Accuracy
Tree-Cycles	0.9123	0.9086
Tree-Grid	0.8434	0.8744
BA-Shapes	0.9661	0.9857

The train, validation, and test datasets are divided into an 80:10:10 ratio. The algorithms run for 1000 epochs with early stopping after 200 patience steps on the validation set. The performance analysis of the base GNN models for each graph classification dataset is presented in Table K.

A.5 Details of Factual Explainers for the Graph Classification Task

In many cases, explainers generate continuous explanations that can be used with graph neural network (GNN) models, which can handle edge weights. To be able to use explanations in our GNN models, we map them into $[0, 1]$ using a sigmoid function if not mapped. While generating performance results, we calculate top-k edges based on their scores instead of assigning a threshold value (e.g., 0.5). However, there are some approaches, such as GEM and SubgraphX, that do not rely on continuous edge explanations.

GEM employs a variational auto-encoder to reconstruct ground truth explanations. As a result, the generated explanations can include negative values. While our experiments primarily focus on the

Table K: Test accuracy of black-box GNN Φ trained for graph classification task, averaged over 10 runs with random seeds. We train multiple GNNs for this task in order to test explainers for stability against GNN architectures.

Dataset	GCN	GAT	GIN	GraphSAGE
Mutagenicity	0.8724 ± 0.0092	0.8685 ± 0.0111	0.8914 ± 0.0101	0.8749 ± 0.0059
Mutag	0.925 ± 0.0414	0.8365 ± 0.0264	0.9542 ± 0.0149	0.8323 ± 0.0445
Proteins	0.8418 ± 0.0144	0.8362 ± 0.0269	0.8352 ± 0.0165	0.8408 ± 0.0124
IMDB-B	0.8318 ± 0.0197	0.8292 ± 0.015	0.8554 ± 0.027	0.8373 ± 0.0093
AIDS	0.999 ± 0.0005	0.9971 ± 0.0068	0.9797 ± 0.0099	0.9903 ± 0.0088
NCI1	0.8243 ± 0.028	0.8096 ± 0.015	0.8365 ± 0.0201	0.8303 ± 0.0137
Graph-SST2	0.957 ± 0.001	0.9603 ± 0.0009	0.9552 ± 0.0014	0.9611 ± 0.0011
DD	0.736 ± 0.0377	0.7312 ± 0.048	0.7693 ± 0.0238	0.7541 ± 0.0415
REDDIT-B	0.8984 ± 0.0247	0.8444 ± 0.0266	0.6886 ± 0.1231	0.8733 ± 0.0196
ogbg-molhiv	0.9729 ± 0.0002	0.9722 ± 0.0010	0.9726 ± 0.0003	0.9725 ± 0.0005

order of explanations and do not require invoking the base GNN in the second stage of GEM, we can still use negative explanation edges.

On the other hand, SubgraphX ranks different subgraph explanations based on their scores. We select the top 20 explanations and, for each explanation, compute the subgraph. Then, we enhance the importance of each edge of a particular subgraph by incrementing its score by 1. Finally, we normalize the weights of the edges. This process allows us to obtain continuous explanations as well.

A.6 Codes and Implementation

Table L shows the code bases we have used for the explainers. We have adapted the codes based on our base GNN models. Our repository, <https://github.com/Armagaan/gnn-x-bench>, includes the adaptations of the methods to our base models.

Table L: Reference of code repositories.

Method	Repository
PGExplainer [30]	https://github.com/LarsHoldijk/RE-ParameterizedExplainerForGraphNeuralNetworks/
TAGExplainer [51]	https://github.com/divelab/DIG/tree/main/dig/xgraph/TAGE/
CF ² [43]	https://github.com/chrisjtann/gnn_cff
RCExplainer [6]	https://developer.huaweicloud.com/develop/aigallery/notebook/detail?id=e41f63d3-e346-4891-bf6a-40e64b4a3278
GNNExplainer [59]	https://github.com/LarsHoldijk/RE-ParameterizedExplainerForGraphNeuralNetworks/
GEM [28]	https://github.com/wanyu-lin/ICML2021-Gem/
SubgraphX [62]	https://github.com/divelab/DIG/tree/main/dig/xgraph/SubgraphX

A.7 Feasibility for Factual Explanations

The feasibility metric is commonly used in the context of counterfactual graph explainers because it measures how feasible it is to achieve a specific counterfactual outcome. In other words, it assesses the likelihood of a counterfactual scenario being realized given the constraints and assumptions of the underlying base model. On the other hand, factual explainers aim to explain why a model makes a certain prediction based on the actual input data. They do not involve any counterfactual scenarios, so the feasibility metric is not relevant in this context. Instead, factual explainers may use other metrics such as sufficiency and reproducibility to provide insights into how the model is making its predictions. Therefore, we have not used feasibility metrics for factual explanations.

B Stability

Stability against feature perturbation: To determine the perturbation amount, we apply the following procedure. For each feature f we compute its standard deviation σ_f . Then we sample a value uniformly at random from $\Delta \sim [-0.1, 0.1]$. The feature value f_x is perturbed to $f_x + \Delta \times \sigma_f$.

Figure F(left inset) illustrates the outcomes, demonstrating a continuation of the previously observed trends. Among these trends, RCEXPLAINER exhibits the highest stability, whereas GNNEXPLAINER displays the lowest stability. This discrepancy in stability could potentially be ascribed to the transductive nature of GNNEXPLAINER, as opposed to the remaining methods, which are all inductive. Transductive methods do not generalize to unseen data and hence when the topology is perturbed, stability suffers. TAGEXPLAINER is task agnostic and hence shows more more instability compared to the other inductive methods.

Adversarial attack on topology: For topology adversarial attack, we follow the flip edge method from [49] with a query size of one. Figure F demonstrates the performance of four factual methods on these evasion attacks. The behavior of the factual methods is similar to the topological noise attack explained in Section 4.2 and the feature perturbations results. When adversarial attack is compared to random perturbations (Fig. 3), we observe higher deterioration in stability, which is expected since adversarial attacks are designed to perturb edges that has higher impact on GNN output.

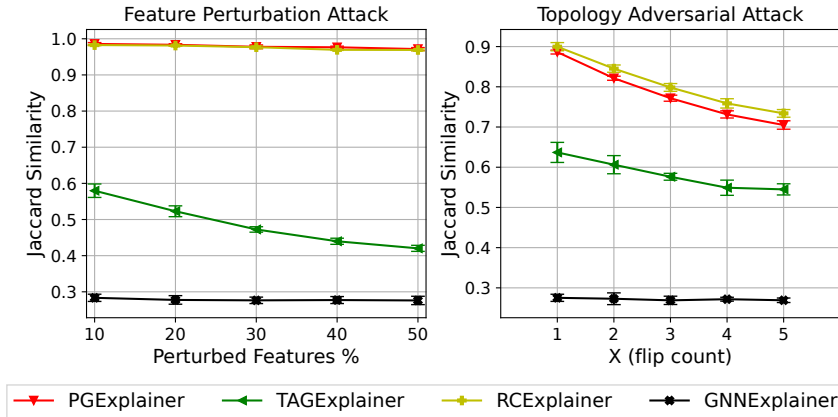


Figure F: Stability of factual explainers in terms of Jaccard similarity of explanations against random feature perturbation (with % in x-axis) and random edge flip (with size in x-axis) on Proteins dataset.

B.1 Counterfactual Explainers

Stability against topological noise: In this section, we investigate the influence of topological noise on datasets on both the performance and generated explanations of counterfactual explainers. For inductive methods (RCEXPLAINER and CLEAR), we utilize explainers trained on noise-free data and only infer on the noisy data. However, for the transductive method CF², we retrain the model using the noisy data.

Figure G presents the average Jaccard similarity results, indicating the similarity between the counterfactual graph predicted as an explanation for the original graph and the noisy graphs at varying levels of perturbations. Additionally, Figure H demonstrates the performance of different explainers in terms of sufficiency and size as the degree of noise increases. This provides insights into how these explainers handle higher levels of noise.

RCEExplainer outperforms other baselines by a significant margin in terms of size and sufficiency across datasets, as shown in Fig. H. However, the Jaccard similarity between RCEExplainer and CF² for counterfactual graphs is nearly identical, as shown in Fig. G. CF² benefits from its transductive training on noisy graphs. CLEAR’s results are not shown for Proteins and Mutagenicity datasets due to scalability issues. In the case of IMDB-B dataset, CLEAR is highly unstable in predicting counterfactual graphs, indicated by a low Jaccard index (Fig. G). Additionally, CLEAR demonstrates high sufficiency but requires a large number of edits, indicating difficulty in finding minimal-edit counterfactuals (Fig. H).

Overall, RCExplainer seems to be the model of choice when topological noise is introduced, and it is significantly faster than CF^2 because it is inductive. Further, it is better than CLEAR as the latter does not scale for larger datasets and is inferior in terms of sufficiency and size as well.

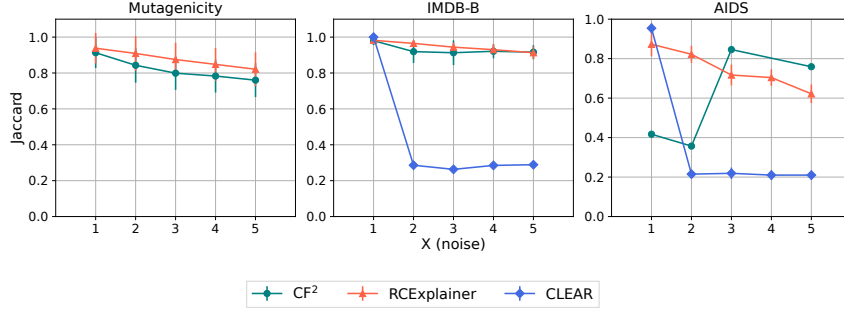


Figure G: Stability of counterfactual explainers against topological noise (Jaccard). We omit CLEAR for Mutagenicity and Proteins as it throws an OOM error for these datasets. The absence of markers representing CF^2 in the Protein dataset’s plot indicates that counterfactual graphs were not predicted at the corresponding noise values by the method. Overall, RCExplainer performs best in terms of the Jaccard index. CF^2 seems to be robust as well, owing to its transductive nature.

Stability against explainer instances: In Table 8, we provide an overview of the stability using *Jaccard index* exhibited among explainer instances trained using three distinct seeds. Similarly, as additional results, here we present the variations in sufficiency (Table M) and the explanation size (Table N) produced by the methods using three different seeds. In terms of sufficiency, the methods show stability while varying the seeds. However, the results are drastically different for explanation size. Table N present the results. We observe that RCExplainer is consistently the most stable method while CF^2 is worse. The worst stability is shown by CLEAR and this observation is consistent with the previous results.

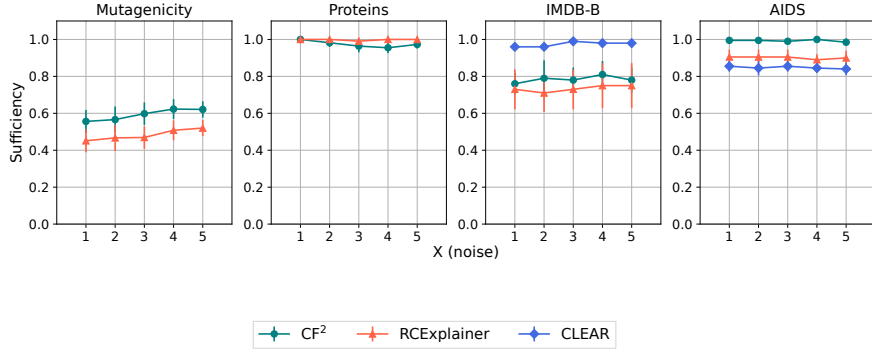
Table M: Stability of sufficiency produced by counterfactual explainers against the explainer instances (seeds). The best explainers for each dataset (row) are highlighted in gray, yellow and cyan shading for seeds 1, 2, and 3, respectively. OOM indicates that the explainer threw an out-of-memory error.

Dataset / Seeds	RCExplainer			CF^2			CLEAR		
	1	2	3	1	2	3	1	2	3
Mutagenicity	0.4 ±0.06	0.40 ±0.05	0.41 ±0.05	0.50 ±0.05	0.49 ±0.06	0.52 ±0.05	OOM	OOM	OOM
Proteins	0.96 ±0.02	0.96 ±0.02	0.96 ±0.02	1.0 ±0.0	1.0 ±0.0	0.98 ±0.02	OOM	OOM	OOM
Mutag	0.4 ±0.12	0.6 ±0.12	0.55 ±0.1	0.9 ±0.12	0.85 ±0.2	0.9 ±0.12	0.55 ±0.1	0.55 ±0.1	0.65 ±0.12
IMDB-B	0.72 ±0.11	0.72 ±0.11	0.72 ±0.11	0.81 ±0.07	0.82 ±0.08	0.81 ±0.07	0.96 ±0.02	0.96 ±0.02	0.96 ±0.02
AIDS	0.91 ±0.04	0.91 ±0.04	0.91 ±0.04	0.98 ±0.02	1.0 ±0.0	0.99 ±0.01	0.84 ±0.03	0.82 ±0.03	0.83 ±0.04
ogbg-molhiv	0.90 ±0.02	0.88 ±0.01	0.90 ±0.01	0.96 ±0.01	0.97 ±0.00	0.96 ±0.00	OOM	OOM	OOM

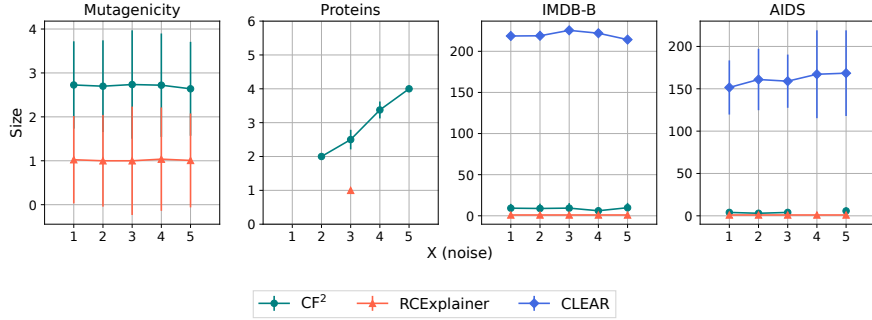
Table N: Stability of *explanation size* produced by explainers against the explainer instances (seeds). NA indicates the inability to find a counterfactual. OOM indicates that the explainer threw out-of-memory error. The best explainers for each dataset (row) are highlighted in gray, yellow and cyan shading for seeds 1, 2, and 3, respectively.

Dataset / Seeds	RCExplainer			CF^2			CLEAR		
	1	2	3	1	2	3	1	2	3
Mutagenicity	1.01 ±0.19	1.0 ±0.0	1.25 ±0.0	2.78 ±0.98	2.85 ±1.07	2.95 ±1.37	OOM	OOM	OOM
Proteins	1.0 ±0.0	1.0 ±0.0	1.0 ±0.0	NA	NA	3.0 ±0.0	OOM	OOM	OOM
Mutag	1.1 ±0.22	1.0 ±0.0	1.0 ±0.0	1.0 ±0.0	1.25 ±0.35	1.0 ±0.0	17.15 ±1.62	15.6 ±1.86	19.05 ±1.31
IMDB-B	1.0 ±0.0	1.0 ±0.0	1.0 ±0.0	8.57 ±4.99	8.29 ±4.50	9.01 ±5.58	218.62 ±0.0	182.25 ±0.0	181.38 ±0.0
AIDS	1.0 ±0.0	1.0 ±0.0	1.0 ±0.0	5.25 ±0.35	NA	6.0 ±0.0	164.95 ±47.93	162.32 ±45.70	185.29 ±78.92
ogbg-molhiv	1.0 ±0.0	1.0 ±0.0	1.02 ±0.42	10.45 ±4.43	9.69 ±4.18	10.24 ±4.87	OOM	OOM	OOM

Stability against GNN architectures: Table O shows the stability of the explainers across different GNN architectures. Similar to our factual setting (Table 7), we assess the stability by computing the Jaccard coefficient between the explained predictions of the indicated GNN architecture and the



(a) Sufficiency



(b) Size

Figure H: Performance evaluation of counterfactual explainers against topological noise. We omit CLEAR for Mutagenicity and Proteins as it throws an OOM error for these datasets. RCEXPLAINER is more robust to noise in both metrics: (a) sufficiency and (b) size.

default GCN model. Unsurprisingly, the stability of the explainer highly depends on the dataset. RCEXPLAINER is also the most stable among all the explainers, and the produced high values indicate that the method is agnostic towards the variations in different message aggregating schemes of the architectures.

We further look into the stability of the counterfactual methods in terms of sufficiency (Table P) and the explanation size (Table Q) across different GNN architectures. The sufficiency results (Table P) show large variations produced by the same method on the same dataset due to the different architectures and message passing schemes. For instance, RCEXPLAINER produces sufficiency of .10 and .93 on the AIDS dataset for GAT and GIN, respectively. In terms of explanation size (Table Q), RCEXPLAINER is stable against different GNN architectures. However, consistent with previous stability results, CF² is more unstable than RCEXPLAINER and the worst stability is shown by CLEAR.

Stability to feature noise: Table R presents the impact of feature noise on counterfactual explanations in Mutag and Mutagenicity. In both datasets, the features are binary in nature. We sample $X\%$ of nodes uniformly at random and flip a randomly sampled feature in this node. We then vary X and measure how stability reacts to the injected noise. We observe that CF² and CLEAR are markedly more stable than RCEXPLAINER in Mutag. This outcome is not surprising, considering that RCEXPLAINER exclusively addresses topological perturbations, while both CF² and CLEAR accommodate perturbations encompassing both topology and features. In Mutagenicity, RCEXPLAINER exhibits slightly higher stability than CF².

Table O: Stability of counterfactual explainers against the GNN architecture. We report the Jaccard coefficient of explanations obtained for GAT, GIN and GRAPHSAGE against the explanation provided over GCN. The higher the Jaccard, the more is the stability. The best explainers for each dataset (row) are highlighted in gray, yellow and cyan shading for architectures GAT, GIN, and GRAPHSAGE, respectively. GRAPHSAGE is denoted by SAGE. NA indicates one or both of the architectures were unable to identify a counterfactual for the graphs. OOM indicates that the explainer threw an out-of-memory error.

Dataset / Architecture	RCExplainer			CF ²			CLEAR		
	GAT	GIN	SAGE	GAT	GIN	SAGE	GAT	GIN	SAGE
Mutagenicity	0.95 \pm 0.05	0.94 \pm 0.06	0.95 \pm 0.03	0.79 \pm 0.13	0.75 \pm 0.16	0.84 \pm 0.10	OOM	OOM	OOM
Proteins	0.88 \pm 0.0	NA	0.88 \pm 0.0	NA	NA	NA	OOM	OOM	OOM
Mutag	0.94 \pm 0.0	NA	0.90 \pm 0.02	NA	NA	NA	0.86 \pm 0.0	NA	0.72 \pm 0.04
IMDB-B	0.99 \pm 0.01	0.98 \pm 0.0	0.98 \pm 0.01	NA	0.93 \pm 0.0	NA	0.60 \pm 0.0	0.70 \pm 0.0	0.76 \pm 0.0
AIDS	0.89 \pm 0.03	NA	NA	0.74 \pm 0.0	0.73 \pm 0.11	0.72 \pm 0.12	0.25 \pm 0.04	0.54 \pm 0.04	0.66 \pm 0.04
ogbg-molhiv	0.96 \pm 0.02	0.96 \pm 0.01	0.96 \pm 0.02	0.63 \pm 0.12	0.13 \pm 0.14	0.61 \pm 0.16	OOM	OOM	OOM

Table P: Stability in terms of *sufficiency* of counterfactual explainers against the GNN architectures. OOM indicates that the explainer threw out-of-memory error. The best explainers for each dataset (row) are highlighted in gray, yellow, cyan, and pink shading for GCN, GAT, GIN, SAGE, respectively. RCExplainer outperforms other baselines on a majority of the datasets and architectures. CLEAR also is stable in terms of sufficiency but has a much larger explanation size compared to other baselines(Refer Table Q).

Dataset / Architecture	RCExplainer				CF ²				CLEAR			
	GCN	GAT	GIN	SAGE	GCN	GAT	GIN	SAGE	GCN	GAT	GIN	SAGE
Mutagenicity	0.4 \pm 0.06	0.38 \pm 0.04	0.6 \pm 0.04	0.59 \pm 0.06	0.50 \pm 0.05	0.64 \pm 0.04	0.57 \pm 0.08	0.62 \pm 0.03	OOM	OOM	OOM	OOM
Proteins	0.96 \pm 0.02	0.88 \pm 0.04	0.3 \pm 0.05	0.46 \pm 0.08	1.0 \pm 0.0	1.0 \pm 0.0	0.76 \pm 0.06	0.79 \pm 0.02	OOM	OOM	OOM	OOM
Mutag	0.4 \pm 0.12	0.7 \pm 0.19	1.0 \pm 0.0	0.45 \pm 0.19	0.9 \pm 0.12	0.9 \pm 0.12	0.45 \pm 0.33	0.7 \pm 0.19	0.55 \pm 0.1	0.8 \pm 0.19	1.0 \pm 0.0	0.05 \pm 0.1
IMDB-B	0.72 \pm 0.11	0.89 \pm 0.02	0.54 \pm 0.06	0.39 \pm 0.04	0.81 \pm 0.07	1.0 \pm 0.0	0.98 \pm 0.02	0.99 \pm 0.02	0.96 \pm 0.02	0.68 \pm 0.08	0.22 \pm 0.11	0.32 \pm 0.11
AIDS	0.91 \pm 0.04	0.10 \pm 0.04	0.93 \pm 0.03	0.86 \pm 0.05	0.98 \pm 0.02	0.92 \pm 0.04	0.96 \pm 0.01	0.96 \pm 0.02	0.84 \pm 0.03	0.80 \pm 0.04	0.74 \pm 0.04	0.84 \pm 0.02
ogbg-molhiv	0.90 \pm 0.02	0.80 \pm 0.01	0.56 \pm 0.01	0.20 \pm 0.01	0.96 \pm 0.01	0.96 \pm 0.01	0.90 \pm 0.01	0.59 \pm 0.01	OOM	OOM	OOM	OOM

C Necessity and Reproducibility for the Factual Explainers: Results for Sec. 4.3

We have defined *Necessity* (inferring on the residual graph obtained after removing the explanation) and (2) *Reproducibility* [26] (retraining the GNN on a subset of residual graphs and then making predictions on the remaining unseen residual graphs) in Sec. 4.3. We present the results here. In both cases, we evaluate performance using sufficiency which in this context, measures the ratio of graphs for which the GNN prediction on the residual graph is the same as in the original graph. After removing the explanation, we expect sufficiency to be low.

The results are presented in Figs. I and J. While sufficiency is indeed low in necessity (Fig. I), this is not the case in reproducibility (Fig. J). These findings suggest that while current factual explainers effectively explain the model, they do not provide a comprehensive explanation of the underlying data. The fact that the GNN can regain prediction accuracy when retrained indicates the presence of other signals that the initial factual explanation failed to capture.

Counterfactual methods. Please note that we have omitted the results for counterfactual methods in Section 4.3. This is because the necessity of counterfactuals is defined as 1-sufficiency, making it a derived metric. To achieve reproducibility, it is necessary to retrain the GNN; however, the label set for counterfactual graphs differs from the one used to train the original black-box GNN. Consequently, comparing their performance becomes impractical.

D Visualization of Explanations

In Figs. K and L, we engage in a visual analysis of the explanations provided by various GNN explainers. The graphs presented in these figures represent mutagenic molecules sourced from the Mutag dataset. Several insights emerge from this analysis.

Factual: The mutagenic attribute of the molecule in Fig. K stems from the presence of the NO₂ group attached to the benzene ring[59, 14]. As a result, the optimal explanation entails pinpointing this specific benzene ring in conjunction with the NO₂ group. Notably, we observe that while certain explainers identify fragments of this subgraph, with CF² achieving the highest overlap, many also highlight bonds originating from regions outside the authentic explanatory context. Adding to the intrigue, the explanation offered by RCExplainer stands out due to its compactness, resulting

Table Q: Stability of *explanation size* produced by explainers against different GNN architectures. OOM indicates that the explainer threw out-of-memory error. NA indicates that the explainer could not identify a counterfactual for the graphs. The best explainers for each dataset (row) are highlighted in gray, yellow, cyan, and pink shading for GCN, GAT, GIN, SAGE respectively. RCExplainer outperforms other counterfactual baselines.

Dataset / Architecture	RCExplainer				CF ²				CLEAR			
	GCN	GAT	GIN	SAGE	GCN	GAT	GIN	SAGE	GCN	GAT	GIN	SAGE
Mutagenicity	1.01 ±0.19	1.36 ±1.46	1.23 ±1.23	1.0 ±0.0	2.78 ±0.98	3.50 ±1.73	6.18 ±3.20	3.27 ±1.51	OOM	OOM	OOM	OOM
Proteins	1.0 ±0.0	1.0 ±0.0	1.0 ±0.0	1.0 ±0.0	NA	NA	3.40 ±1.48	1.92 ±0.71	OOM	OOM	OOM	OOM
Mutag	1.1 ±0.22	1.0 ±0.0	NA	1.0 ±0.0	1.0 ±0.0	1.0 ±0.0	19.38 ±1.03	2.0 ±0.0	17.15 ±1.62	16.5 ±1.44	NA	19.11 ±3.28
IMDB-B	1.0 ±0.0	1.0 ±0.0	1.0 ±0.0	1.0 ±0.0	8.57 ±4.99	NA	6.0 ±0.0	10.0 ±0.0	218.62 ±0.0	343.02 ±49.16	344.32 ±86.03	247.51 ±56.72
AIDS	1.0 ±0.0	1.0 ±0.0	1.0 ±0.0	1.0 ±0.0	5.25 ±0.35	3.60 ±1.57	2.0 ±0.0	2.25 ±0.64	164.95 ±47.93	577.46 ±88.55	161.34 ±40.94	136.68 ±29.34
ogbg-molhiv	1.0 ±0.0	1.0 ±0.0	1.0 ±0.0	1.0 ±0.0	10.45 ±4.43	7.58 ±4.09	21.92 ±11.60	5.46 ±2.17	OOM	OOM	OOM	OOM

Table R: Stability of counterfactual explainers against feature perturbation on “Mutag” and “Mutagenicity” datasets. We do not report results for CLEAR on Mutagenicity since it runs out of GPU memory.

(a) Mutag

Noise% / Metric	RCExplainer			CF ²			CLEAR		
	Sufficiency	Size	Jaccard	Sufficiency	Size	Jaccard	Sufficiency	Size	Jaccard
0 (no noise)	0.4 ±0.12	1.10 ±0.22	1.0 ±0.0	0.90 ±0.12	1.0 ±0.0	1.0 ±0.0	0.55 ±0.1	17.15 ±1.62	1.0 ±0.0
10	1.0 ±0.0	NA	NA	0.6 ±0.2	2.17 ±0.31	0.19 ±0.0	0.55 ±0.1	16.35 ±1.68	0.98 ±0.01
20	0.75 ±0.22	1.0 ±0.0	NA	0.25 ±0.16	1.95 ±0.80	NA	0.55 ±0.1	18.1 ±1.94	0.55 ±0.01
30	1.0 ±0.0	NA	NA	0.6 ±0.3	1.0 ±0.0	0.29 ±0.0	0.55 ±0.1	19.1 ±2.91	0.57 ±0.02
40	1.0 ±0.0	NA	NA	0.6 ±0.2	2.8 ±0.0	0.29 ±0.0	0.55 ±0.1	14.7 ±1.78	0.58 ±0.02
50	1.0 ±0.0	NA	NA	0.8 ±0.1	1.5 ±0.0	NA	0.55 ±0.1	16.05 ±2.48	0.54 ±0.02

(b) Mutagenicity

Noise% / Metric	RCExplainer			CF ²		
	Sufficiency	Size	Jaccard	Sufficiency	Size	Jaccard
0 (no noise)	0.4 ±0.06	1.01 ±0.19	1.0 ±0.0	0.50 ±0.05	2.78 ±0.98	1.0 ±0.0
10	0.43 ±0.04	1.01 ±0.19	0.96 ±0.04	0.49 ±0.04	2.11 ±1.06	0.92 ±0.06
20	0.47 ±0.06	1.0 ±0.0	0.95 ±0.04	0.53 ±0.06	1.73 ±0.94	0.86 ±0.08
30	0.50 ±0.04	1.0 ±0.0	0.94 ±0.04	0.61 ±0.04	1.68 ±0.91	0.86 ±0.09
40	0.52 ±0.05	1.0 ±0.0	0.93 ±0.06	0.54 ±0.05	1.47 ±0.73	0.87 ±0.09
50	0.49 ±0.05	1.0 ±0.0	0.93 ±0.06	0.67 ±0.01	1.54 ±1.06	0.86 ±0.08

in commendable statistical performance. However, this succinct explanation lacks meaning in the eyes of a domain expert. Consequently, a pressing need arises for real-world datasets endowed with ground truth explanations, a resource that the current field unfortunately lacks.

Counterfactuals: Fig. L illustrates two molecules, with Molecule 1 (top row) being identical to the one shown in Fig. K. The optimal explanation involves eliminating the NO₂ component, a task accomplished solely by CF² in the case of Molecule 1. While the remaining explanation methods can indeed alter the GNN prediction by implementing the changes described in Figure L, two critical insights emerge. First, statistically, RCEXPLAINER is considered a better explanation than CF² since its size is 1 compared to 3 of CF². However, our interaction with multiple chemists clearly indicated their preference towards CF² since eliminates the entire NO₂ group. Second, chemically infeasible explanations are common as evident from CLEAR for both molecules and CF² in molecule 2. Both fail to adhere to valency rules, a behavior also noted in Sec. 4.4.

E Additional Experiments on Sparsity Metric

Counterfactual explainers: Sparsity is defined as the proportion of edges from the graph that is retained in the counter-factual [61]; a value close to 1 is desired. In node classification, we compute this proportion for edges in the \mathcal{N}_v^ℓ , i.e., the ℓ -hop neighbourhood of the target node v . We present the results on sparsity metric on node and graph classification tasks in Table S and T, respectively. For node classification, we see CF-GNNEXPLOINER continues to outperform (Table S). The results are

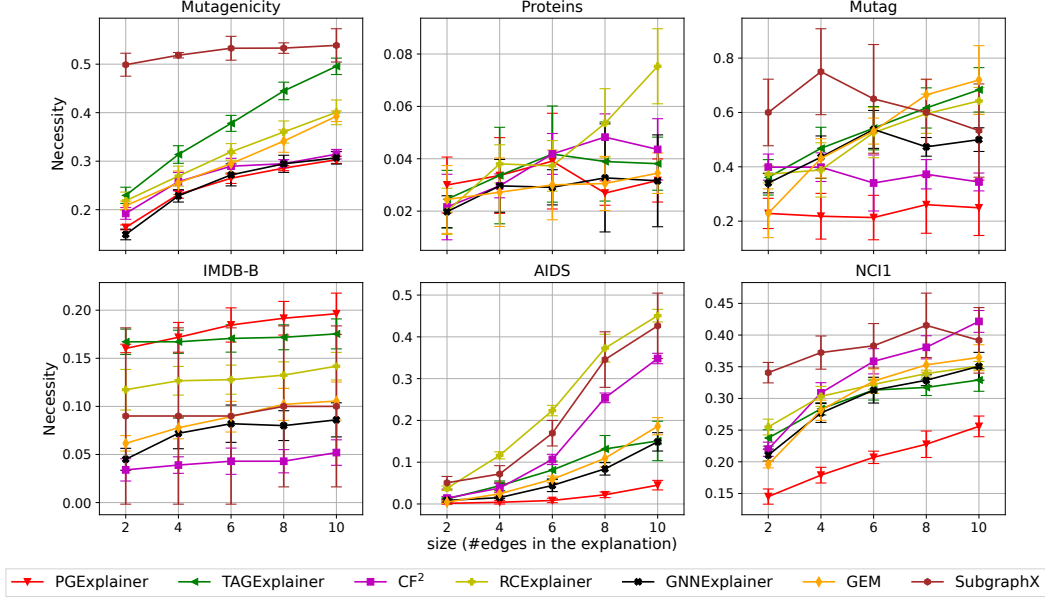


Figure I: Necessity (in terms of sufficiency) of various factual explainers against the explanation size. Necessity is inferring on the residual graph obtained after removing the explanation. We evaluate performance using sufficiency which is the ratio of the GNN prediction on the residual graph (after the explanation removal) and on the original graph.

consistent with our earlier results in Table 5. Similarly, Table T shows that RCEExplainer continues to outperform in the case of graph classification (earlier results show a similar trend in Table 4).

Factual explainers: For experiments with factual explainers, we report results of the necessity metric on varying degrees of sparsity (Recall Fig. I). Note that size acts as a proxy for sparsity in this case. This is because sparsity only involves the normalized size where it is normalized by the number of total edges. So sparsity can be obtained by normalizing all perturbation sizes in the plots to get the sparsity metric. For counterfactual explainers, we do not supply explanation size as a parameter. Hence, computing the sparsity of the predicted counterfactual becomes relevant.

Table S: Results on sparsity of counterfactual explainers for node classification. CF-GNNExplainer consistently produces the best results that are shown in gray.

Method/Dataset	Tree-Cycles	Tree-Grid	BA-Shapes
CF-GNNEXPLAINER	0.93 \pm 0.02	0.95 \pm 0.03	0.99 \pm 0.00
CF ²	0.52 \pm 0.14	0.58 \pm 0.14	0.99 \pm 0.00

Table T: Results on sparsity of counterfactual explainers for graph classification. Best results are shown in gray. RCEXPLAINER consistently outperforms the other methods.

Method/Dataset	Mutagenicity	Mutag	Proteins	AIDS	IMDB-B	ogbg-molhiv
RCEExplainer	0.96 \pm 0.00	0.94 \pm 0.01	0.94 \pm 0.02	0.91 \pm 0.00	0.98 \pm 0.00	0.96 \pm 0.00
CF ²	0.90 \pm 0.01	0.94 \pm 0.0	NA	0.99 \pm 0.01	0.89 \pm 0.04	0.62 \pm 0.05
CLEAR	OOM	0.88 \pm 0.07	OOM	0.66 \pm 0.04	0.87 \pm 0.06	OOM

F TAGExplainer Variants

TAGExplainer has two stages. We define TAGExplainer (1) as when we apply only the first stage and get explanations, whereas TAGExplainer (2) applies both stages. Figure M compares performance of these two variants.

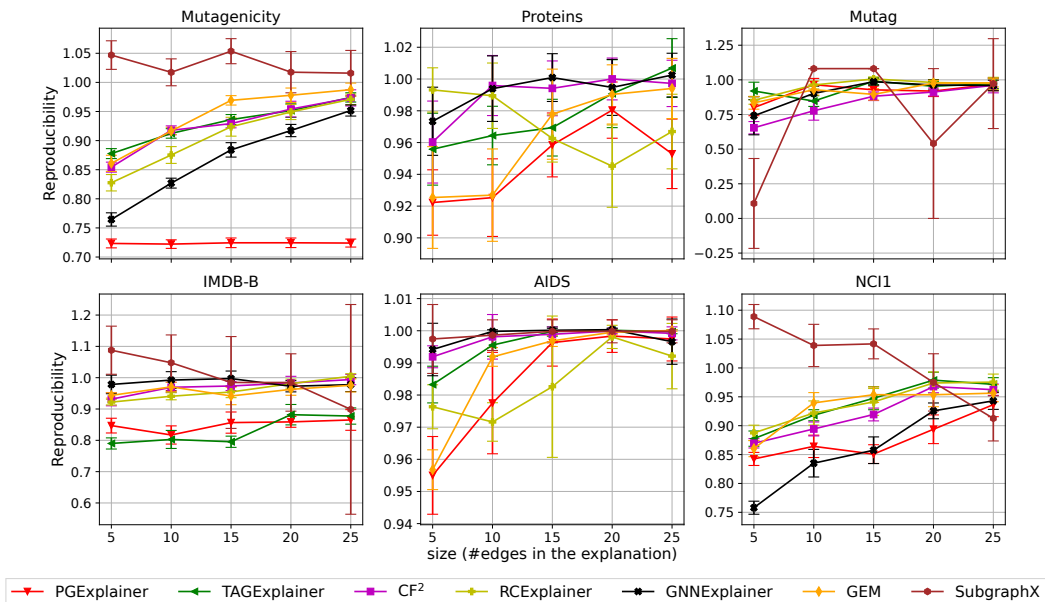


Figure J: Reproducibility (in terms of sufficiency) of factual explainers against size. Reproducibility is retraining the GNN on a subset of residual graphs and then making predictions on the remaining unseen residual graphs.

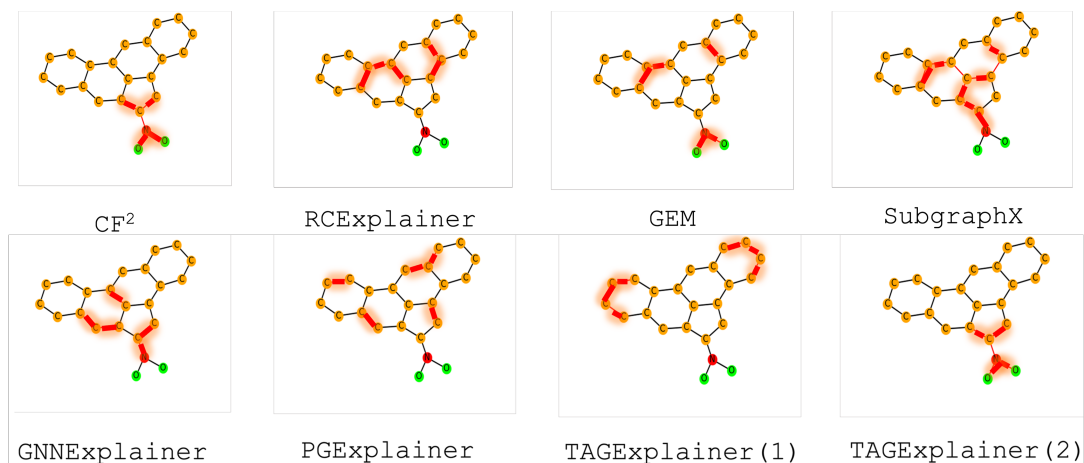


Figure K: Visualization of factual explanations on a mutagenic molecule from the Mutag dataset. The explanations contain the edges highlighted in red.

G Factual Explainers on OGBG-Molhiv

Figure O demonstrates a new dataset OGBG-Molhiv for three factual explainers. On this dataset, three factual methods are close to each other in terms of sufficiency performance.

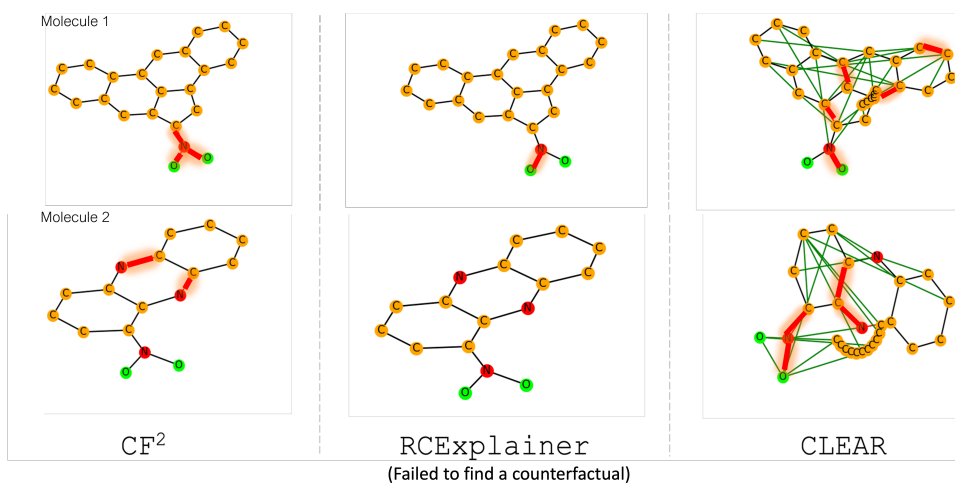


Figure L: Visualization of counterfactual explanations on Mutag dataset. Edge additions and deletions are represented by green and red colors respectively.

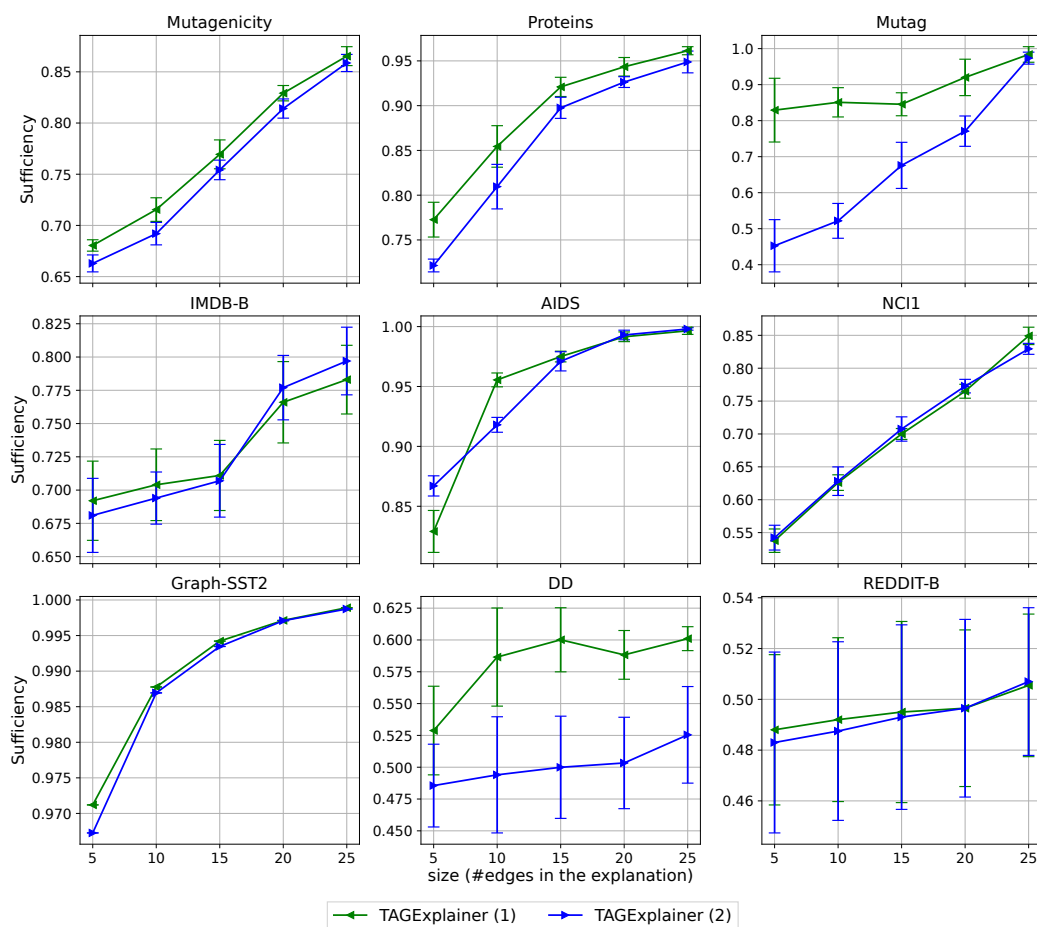


Figure M: Sufficiency of TAGExplainer variants against size. Applying the second stage does not help much for TAGExplainer.

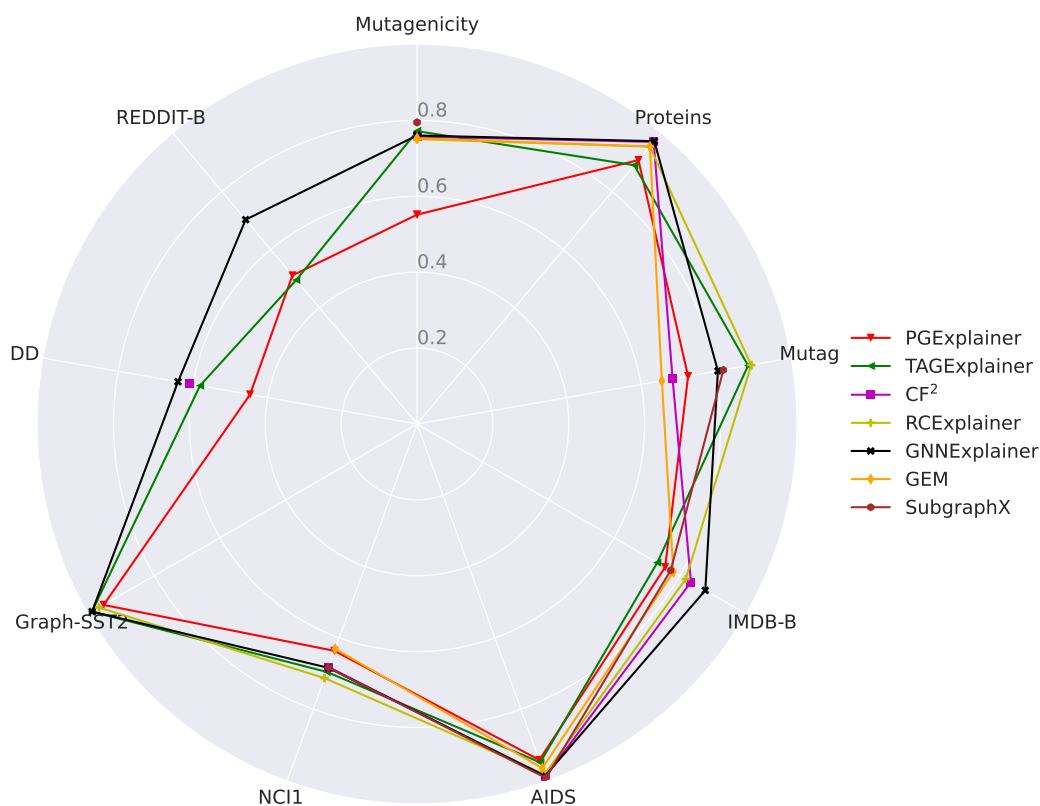


Figure N: Spiderplot for sufficiency performance averaged for different sizes of explanations. Even though there is no clear winner method, GNNEXPLAINER and RCExplainer appear among the top performers in the majority of the datasets. We omit those methods for a dataset that throw an out-of-memory (OOM) error and are not scalable.

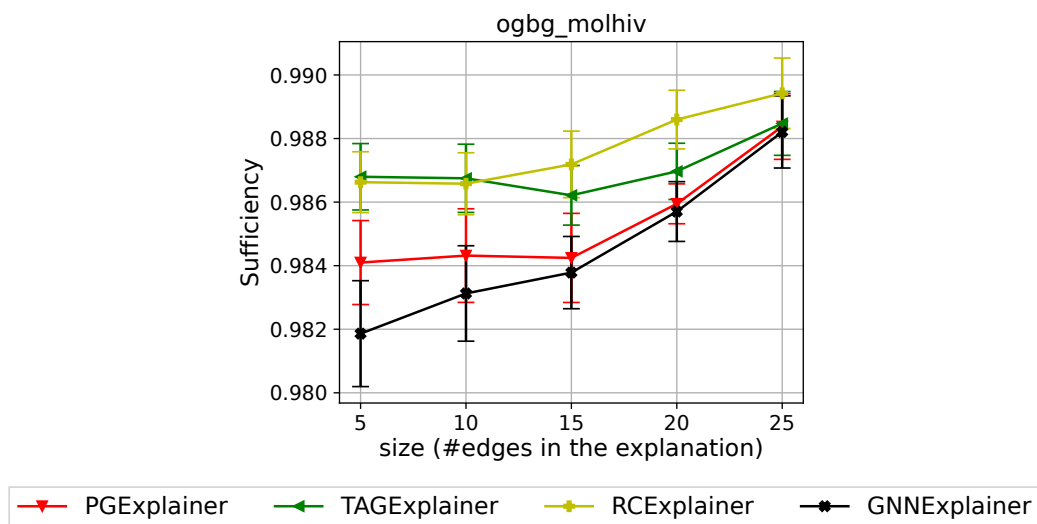


Figure O: Sufficiency of the factual explainer against the explanation size for ogbg-molhiv dataset.